POLITECNICO
MILANO 1863

SCUOLA DI INGEGNERIA INDUSTRIALE
E DELL'INFORMAZIONE

New Equivalent Static Load generation procedure for the vehicle chassis deformability analysis

Tesi di Laurea Magistrale in
Ingegneria Meccanica

Author: **Luiz Felipe Faria Ricardo**

Student ID: 995871
Advisor: Prof. Federico Cheli(Politecnico di Milano)
Co-advisors: Eng. Jens Weber (CEVT), Prof. Michele Vignati (Politecnico di Milano)
Academic Year: 2022-23

Abstract

By Analyzing the dynamic distortion in all body closures openings in a complete vehicle, a better understanding of the body characteristics can be achieved compared to traditional load cases such as static torsional body stiffness. This is particularly relevant for non-traditional vehicle layouts and electric vehicle architectures. The body response is measured with the Multi Stethoscope (MSS) when driving on a pavé road (cobblestone). The MSS measures the distortion in each opening in two diagonals. During the virtual development, the distortion is described by the relative displacement in the diagonal direction in the time domain using a modal transient analysis. The results are shown as Opening Distortion Fingerprint ODF and used as assessment criteria within Solidity and Perceived Quality. By applying the Principal Component Analysis (PCA) to the history of the distortion, a Dominant Distortion Pattern ((DDP) can be identified. The DDP means that more than 50% of the body deformation states for a given pavè time history are similar to each other. This work will present a deeper analysis of the forces which are associated with this Dominant Distortion Pattern (DDP). The analysis includes all forces between the wheel suspension and the trimmed body. Based on the results of this force analysis, a new procedure for creating an Equivalent Static Load (ESL) was developed and is already being applied at CEVT.

Keywords: Complete Vehicle Simulation, vehicle body stiffness, Opening Distortion Fingerprint ODF, Equivalent Static Load ESL, Multi Stethoscope MSS

List of Figures

Contents

Introduction

The development time available for conceiving a vehicle is getting shorter and shorter. By using a range of load cases combined with the right tools, we can reduce the required time to perform a task. Simplifications based on reasonable hypotheses are another way to reduce the complexity of given problems.

A significant part of the development time available is spent on various verification tests. Computer Aided Engineering (CAE) tools are used today in Research and Development ($R\&D$) to reduce the number of physical tests using simulations instead of doing them [9].

Nowadays, reducing development time by using CAE is indispensable in the automotive industry, it can be used for durability [17] and fatigue [21] analyses, NVH [22], crash (vehicle safety) [7], virtual prototyping [33], structural optimization [11] and much more [1, 15, 16, 26, 28, 29].

In the past, the static torsional requirement was arguably the most important structural requirement, for several years it was used as an important reference. Today, body stiffness has taken that position; however, the requirement has to be improved for electrical vehicles, thus becoming even more relevant, the reason being that the heavy and stiff battery pack has a big influence on the overall stiffness of the body.

An important aspect to mention is that instead of obtaining a static value from a unitary torsion, for example, a better understanding of the dynamics of the vehicle is required to correctly assess the body stiffness. The Opening Distortion Fingerprint (ODF) is a tool that provides a global (and dynamic) overview of the distortions in the openings, which will be explored and used in this work, as well as explained in the methodology chapter.

Such a requirement can be studied greatly correlated with the random excitation provided by a vehicle driving Belgium pavé. Studying this scenario is relevant since it simulates a random road profile and is also widely used for vehicle ride quality estimation, an important design parameter, and, of course, allows us to develop a car with high body stiffness. As a consequence, the response of the suspension and the vehicle as a whole

is also random, although the good accuracy of multi-body simulations with experimental data can be achieved once the road profile is known [12], by mapping the test track surface, for example. Forces calculated by ADAMS through this simulation are reliable and used as input for the Finite Element(FE) simulations.

This research will focus on understanding how the forces affect the distortions of the structure and how the deformation patterns *i.e.* deformations of the body at various time steps that share similarities, can be used to simplify the large load history to a few single load cases that represent the general behavior of the structure and that can be used as a quality parameter for any development phase of the vehicle as well as a tool to save a considerable amount of simulation time.

This work will be presented the state of the art for Equivalent Static Load (ESL) which, in this case, will be a reduction of the large load histories to a single static load case, with some additional explanations required as background to further understand the FEM approach that will be used. Followed by the methodology involved in the FE model and post-processing as well as the numerous steps that are included in it. Once everything has been explained, results will be presented along with critical engineering analysis, confirmation of hypotheses will also be present, discussion and conclusions will follow as well as suggestions for future works.

For dynamic simulations of this nature, the modal transient analysis (SOL 112 in Nastran) can be considered overkill, given that no strong dynamic effects take place, but it is convenient to provide results for multiple load cases (each time step). The downside of this method is that around 90% of the simulation time is due to the calculation of eigenmodes. If no considerable dynamic effects take place, performing a linear static analysis can be a reasonable simplification that besides being significantly faster will also provide smaller output files, increasing speed for post-processing operations. In any case, the premise that no strong dynamic effect takes place will be demonstrated in the methodology and results section.

The outcome of the work will be the development of a simplified, but yet consistent, fast, and accurate method of determining the severity of the impact of the forces in the overall deformation of a vehicle, especially in the openings of the body, which will also serve as a quality parameter and have applications in durability and solidity.

The division of this work began with this first chapter; the introduction; followed by chapter 2, the state of the art, where its discussed the most advanced techniques used in this field of study, most specifically using the Equivalent Static Load Method (ESLM) to reduce simulation time while being able to measure the distortions in the openings of the

vehicle, the downsides of the state of the art method will also be pointed out, providing a direction for this work to follow. After that, in chapter 3 the methodology employed and some background knowledge required to fully understand some topics of this work will be provided. Once the methods are described, chapter 4, which contains the results section of this work, will present the numerical results and discuss the outcomes. Despite discussions already being provided in the results chapter, a specific section for discussion is devoted for general discuss on the applicability of the shown method as well as to recap the steps of the proposed method. Finally a conclusion chapter summarizes the achievements and innovative aspects of the proposed methodology.

1 | State of the art

The Equivalent Static Load Method(ESLM) has been extensively used in various fields, such as structural optimization [6, 23, 24], simplification of complex loads [3, 4], vehicle components durability [30], crash optimization [20] and much more [10, 18, 19, 34].

The principle of ESLM consists in optimizing a dynamic load case to a static load case in a way that the displacements obtained is equivalent, justifying the employment of the name Equivalent Static Load. This method has been explained and debated in multiple works [5, 6, 13, 23, 27], and extensive studies have led to a solid, yet expandable understanding of this topic.

Choi and Park described with many details and possible approaches of transforming dynamic loads to static loads from a numerical point of view [6] *i.e.* numerically obtaining the same displacements from equivalent static forces applied in the same force locations, although physically representing different problems.

The most common application of ESLM is structural optimization, which will be explained in further detail, as well as important modifications of the method in relation to the method employed in this work. This work will also use the same reference as Choi and Park regarding the definition of an ESL: "An ESL is defined as a static load which makes the same displacement field as that under a dynamic load at an arbitrary time".

The described procedure has already been validated many times, as already explained. Using vibration theory with finite element methods (FEM), the non linear dynamic response of a structure is expressed accordingly to the equation 1.1 [2].

$$\mathbf{M}(\mathbf{b})\ddot{z}_N(t) + \mathbf{C}(\mathbf{b})\dot{z}_N(t) + \mathbf{K_N}(b, z_N(t))z_N(t) = \mathbf{f(t)} \tag{1.1}$$

Where $\mathbf{M}$ is the mass matrix, $\mathbf{C}$ is the damping matrix, $\mathbf{K}$ is the stiffness matrix, both the matrix being a function of the design variable $\mathbf{b}$, $\mathbf{f}$ being the vector of external dynamic loads, $\mathbf{z}$ is the dynamic displacement field. Two subscripts notation will be used here: $\mathbf{N}$ means that the response (displacement) is obtained by non-linear analysis, whereas $\mathbf{L}$

means that the response(displacement as well) is obtained by linear analysis.

It must be pointed out that **M** and **C** are functions of the design parameter **b**. For instance, the thickness of a component, its cross-sectional shape and the material properties or any other dimension or even the weight of the structure are of course related with the mass and damping matrices, this is even more clear when we think of a one degree of freedom problem, such as a mass-spring-damper system, where the mass matrix is the mass attached to the spring and damper, and is obviously dependent of the material property, the damping matrix is the damping coefficient of the damper and the stiffness matrix is the stiffness of the spring.

Now we focus on the static analysis, where the derivatives in respect to time are null. We already know the deformation history from the nonlinear dynamic analysis z_N, we want to generate the same displacement field z_N from an equivalent static load $f_{eq}(s)$ (instead of f(t)) where **s** relates to a specific time in the load history, the reason for not using t instead is because since we are now working with a static load, that is not time dependent, it would be inconsistent to associate a static analysis with time.

In that case, we take a look at equation 1.2 and see that K_L is the equivalent stiffness matrix for the static analysis, we calculate it from $K_{\mathbf{N}}(b, z_N(t))$ (which means they are the same) for the given time step (associated with **s**). We will also be using the i^{th} superscript to describe that our $f_{eq}(s)$ is associated with the i^{th} time step from our dynamic load history, basically we are taking a picture of that instant and making our analysis with only the information about that specific i^{th} time step.

$$f_{eq}^{i}(s) = K_L z_N^{i}(t) \tag{1.2}$$

Through equation 1.3 we get the relation between the ESL and the dynamic load, where the notation **s** is exactly matched with **t**. It must be emphasized; once more; that the reason for using the notation **s** is that the left side of equations 1.2 and 1.3 are not defined in a dynamic region but in a static region. In other words, t = t_i is equal to s = s_i and the total number of s is n, where n is the total number of time steps from t_i to t_n. Therefore, **n** ESLs are obtained from 1.3. This means that for each time step, we can generate an equivalent static load that after a static analysis will produce the same displacement field, at the equivalent time step, from the non-linear analysis.

$$f_{eq}^{i}(s) = \mathbf{f(t)} - \mathbf{M(b)}\ddot{z}_N(t) + \mathbf{C(b)}\dot{z}_N(t) \tag{1.3}$$

Note that the stiffness matrices are not present anymore in equation 1.3 the reason is that by definition the terms containing the stiffness matrices and displacements are the same in equations 1.1 and 1.2, so by saying that those terms are equal, we finally obtained the equation 1.3.

For a simplified model, not considering the damping effect on the structure *i.e.* neglecting **C**, the optimization procedure with a general goal *e.g.* minimizing weight, and a given tolerance ϵ for **b** can be written according to [24]:

1. Set initial design variables and parameters (cycle number (iteration): k = 0, design variables $b^k = b^0$).
2. Perform a non-linear static analysis with b^k.
3. Calculate the equivalent static load sets.
4. Solve the linear static response optimization problem with the equivalent load sets.
5. When k = 0, go to Step 6. When k > 0, if $||b^k - b^{k-1}|| \leq \epsilon$, then terminate the process. Otherwise, go to Step 6.
6. Update the design results, set k = k + 1 and go to Step 2

A graphical representation of the given algorithm can be seen at figure 1.1.

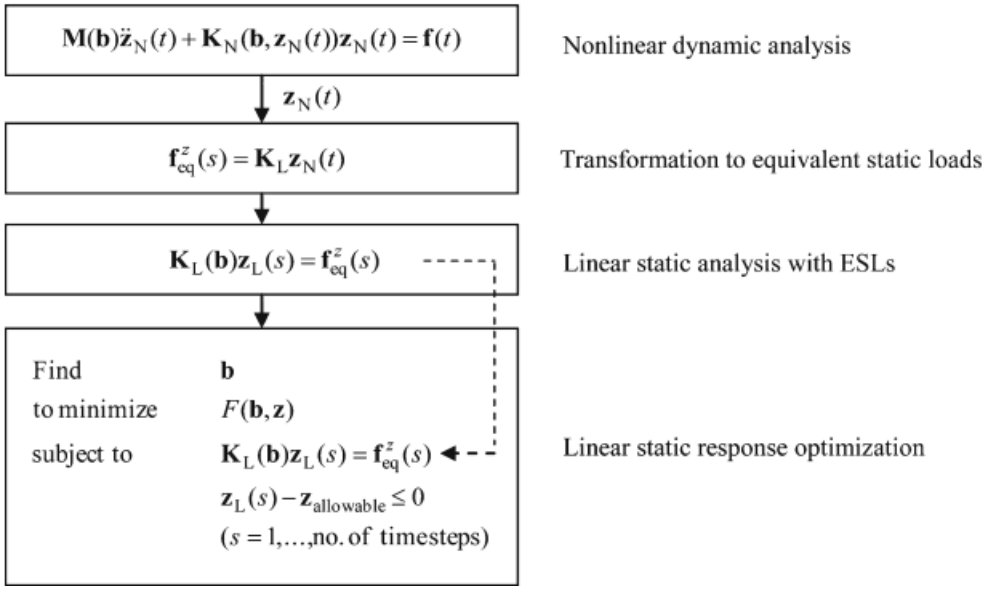

Figure 1.1: Generation of equivalent static loads for displacement [24]

1.1. ESLM at CEVT

Such optimization model has been used by CEVT around 2020 and was a big motivation for the company to improve this past model in terms of accuracy, complexity and time consumption. The reason for creating an ESL was to have a simplified static load case, that could represent the displacements from a dynamic complete vehicle simulation [13, 14] using a simpler model without constraints (also-called free-free analysis using the "inertia relief" parameter in Nastran).

This model consisted in applying 4 forces, one on each top mount of a conventional vehicle and analyzing the relative displacement between both nodes of each diagonal for some of the openings of the vehicle, such as front and rear doors, sun roof and tailgate, see figure 1.2. Not all of the diagonals are represented here for the simplicity of the view, making it easier to understand the concepts that will be further used here. In the figure a few of the most obvious openings in the vehicle are shown, in figure 3.5 in the results section, all of them will be shown.

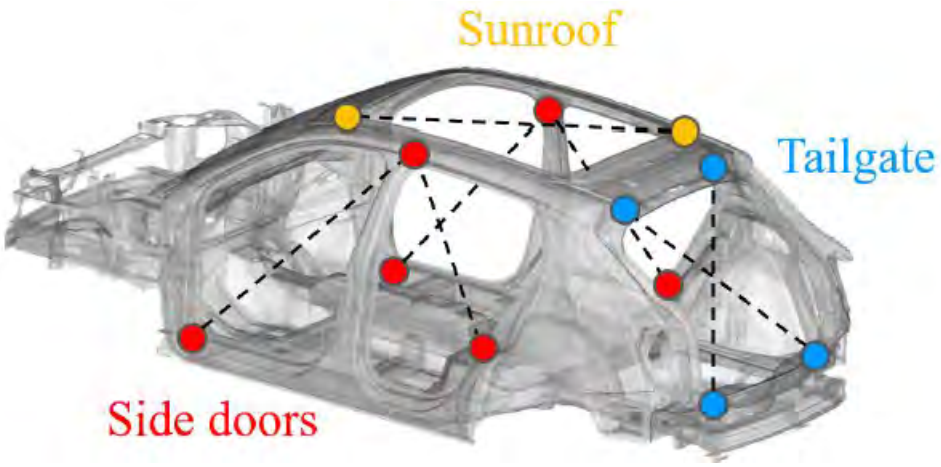

Figure 1.2: Whole vehicle that is used for both static and dynamic simulations, where diagonals in the openings of the vehicle are shown. The ones represented by red dots are associated with the side doors, sunroof by the yellow dots and tailgate by blue dots.

At each time step, for each diagonal in the vehicle, it is defined a constant called U_{SEP}, that is a reference and a representative relative displacement of the two nodes that define a diagonal in the model, for this given scenario, it represents the displacement field for the whole vehicle for the specific time step where the vehicle is under the most critical deformation state, this analysis will be further exploited and explained in section 2.7. U_{ESL}, on the other hand is the parameter of the optimization procedure. And the goal of the optimization is to obtain a variable U_{ESL} very close to U_{SEP}, given a tolerance ϵ.

The objective of the problem is therefore to minimize the difference between those two values, meaning that from the obtained f_{eq} we manage to obtain the same displacement field, or at least very close to it.

On a multiple DOF system, such as multiple openings(and diagonals) in a vehicle, the task of optimization does not become so trivial because of the coupling between different DOFs, as well as the existence of an overdeterminated system, that is not necessarily a determined equation system, given that the number of DOFs could be different from the number of forces that can be controlled, in fact, for the aforementioned case, 12 forces (4 forces with X,Y and Z components) can be controlled, but 12 diagonals (each diagonal associated with 2 distinct nodes with X,Y and Z component) leads to an underdeterminated system, where optimization is still a fair choice to approximate a solution.

Therefore, we have that U_{ESL} is a constant, U_{ESP} is a function of the applied forces, the constraints c(F) are also a function of the applied forces, and the limit that the forces might achieve *e.g.* F at the 4 top mounts, should be bellow a reasonable value not to generate a critical stresses in the structure, therefore this limitation generates a new set of constraints. In summary, the optimization procedure can be define as:

- Minimizing $U_{ESL} - U_{ESP}(F)$
- Subjected to $c(F) \leq 0$

A proposed alternative, which was employed was to consider the magnitude of the relative displacement in each diagonals at each node, modifying the optimization procedure to:

- Minimizing $Di_{ESL} - Di_{ESP}(F)$
- Subjected to $c(F) \leq 0$

Where $Di = \sqrt{(x_2^2 - x_1^2)^2 + (y_2^2 - y_1^2)^2 + (z_2^2 - z_1^2)^2}$ is the relative displacement between two points in a opening, with coordinates (x_1, y_1, y_2) and (x_2, y_2, z_2) respectively. In both cases, our optimization problem is focused on the forces that minimizes the error in the Displacement Di for all openings in the vehicle.

Once the algorithm converges, a comparison can be made between this ESL simulation in respect to the dynamic simulation represented by the average of the displacements Di leading to 30% of the highest distortions in the openings of the vehicle, this concept will be further explored in the section 2.7 in the methodology chapter.

For the following example, a conventional vehicle traveling at 50 km/h on the Belgian pavé (PAV), a clearly dynamic road profile that resembles nearly random road profiles, can be seen in Figure 1.3, showing a good correlation of the results *i.e.* that the ESLs

were able to capture dynamic events. The blue bars represent the relative displacement for each opening, when calculating the average of the 30% highest distortions, while the red bars are representing the relative displacement of all analyzed diagonals as well, but for a specific static load case.

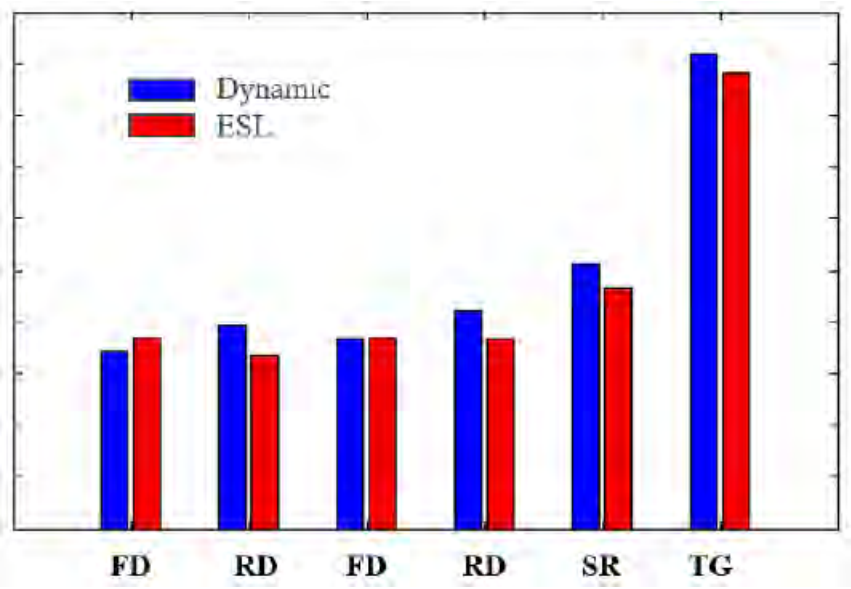

Figure 1.3: Comparing opening distortion (mm) from ESL (red bars) with SEP from dynamic complete vehicle simulation for different openings (blue bars).

Although this method succeeds in obtaining a simplified load that provides an accurate measure of the distortion in the openings of the vehicle as seen in figure 1.3, when comparing the proposed ESL with the dynamic results, it has some downfalls:

- It does not explain why such loads are representative of the given problem.
- It oversimplifies the high complexity of the forces on the vehicle, by reducing all force locations to only the 4 top mounts, neglecting lateral forces.
- It requires a complete dynamic simulation to use its results as target for the optimization problem, thus not being able to anticipate which loads would achieve accurate results beforehand.

2 | Methodology

The vehicle used for this study is the *Lynk & Co 01*, a 5-door compact crossover SUV and is the first model announced from the Chinese brand *Lynk & Co 01*, a brand created by CEVT. The vehicle can be seen in figure 2.1. For future reference, it is worth noting that this work will be focused on a non-conventional vehicle *i.e.* a vehicle with a heavy and stiff battery.

Figure 2.1: Lynk & Co 01

2.1. Distortion in the body openings

First of all, we describe the openings of the vehicle that will be interesting from this analysis perspective, which are: the front and rear doors, tailgate, rear seat, and sunroof; as well as the external forces applied to the body of the vehicle. This can be seen in figure 2.2, where both left doors are represented by two pairs of crossed red diagonals, both right doors by two pairs of crossed black diagonals, the sunroof by a pair of green diagonals, and tailgate and rear seat by two pairs of yellow diagonals. More than that, all force locations are represented by three unitary force vectors in x,y and z, since all forces are input in the Finite Element Solver as a combination of three unidirectional forces. In total we have 8 force locations in the front and 10 in the rear of the vehicle, giving a total of 18 force locations and 54 force directions.

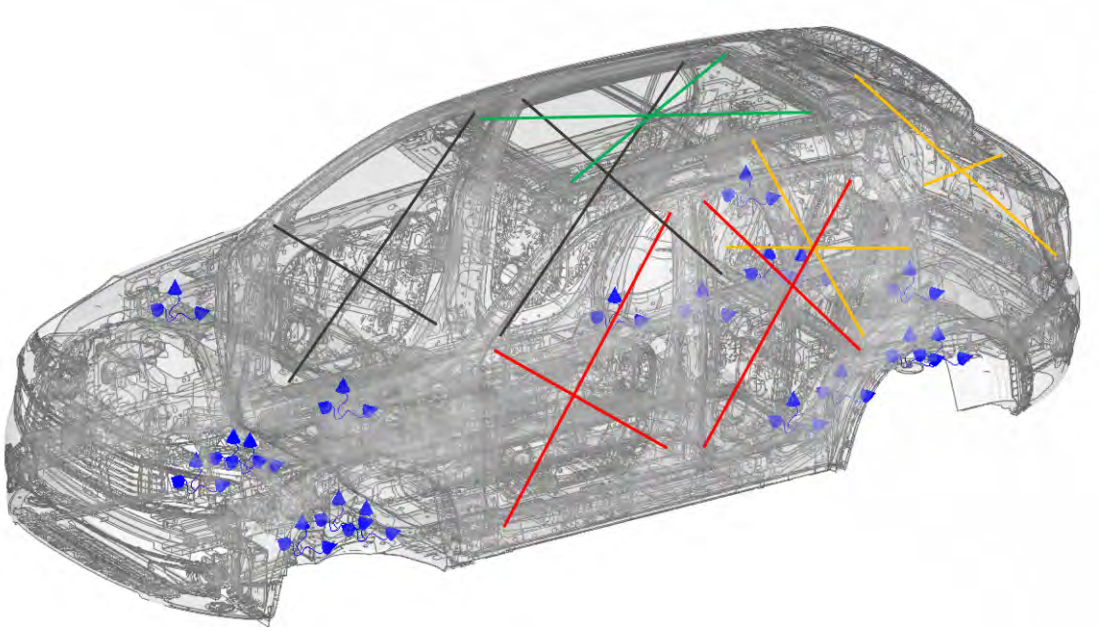

Figure 2.2: All 7 Openings of the vehicle with its 14 diagonals, with red representing the left doors, black the right doors, green the sunroof and yellow the tailgate and rear seat. All 18 force locations are represented by their three unidirectional forces applied on it, they can be seen by unitary vectors painted blue associated with a single point in the vehicle.

2.2. Quasi-static assumption and post-processing of experimental data

Instead of using large load histories for dynamic simulations, such as transient modal analysis (SOL 112 in NASTRAN), if the hypothesis of quasi-static regime is satisfied *i.e.* the system is in equilibrium or very close to it during the whole analyzed time, then the solution of each time step of SOL 112 can be approximated to a linear static analysis (SOL 101 in NASTRAN) with a single static load case, decreasing the complexity of the problem and the required time to solve the matrix problem given by finite element methods (FEM). This would not be true if the excitation of the wheels were close to the body modes that contribute to the distortion of the body.

In theory, the optimization procedure described in chapter 1 could be applied. It comes as no surprise that ESLM requires optimization procedures that will produce ESLs that will be faster to process than dynamic analysis, simply to the fact of the complexity and additional matrix (**M** and **C**) for the FE model. The reason why adding mass and damping matrix adds time to the simulation is because when performing the modal transient analysis, about 80% of the simulation time is focused on inverting matrices and calculating eigenvectors which are heavy computational procedures. Instead of doing so, we aim to perform a linear static analysis, where only the stiffness matrix has to be inverted for each time step, the complexity of the matrix is also smaller than when introducing specially the damping matrix which often contains several off diagonal terms that increases the computational power to perform the required operations, besides that, no modal calculation is required, making it interesting to perform a static analysis instead of a modal analysis, when possible.

On the other hand, optimization itself is also a procedure that takes time, which should also be considered when analyzing how much computational time was saved after the whole procedure. An alternative is proposed for the current work which corresponds to dismembering each time step from the numerous dynamic load cases as equally numerous single static load cases, under the assumption of quasi-static response.

The total movement of the vehicle can be described as the superposition of both rigid body movement and structural deformation. However, rigid body movement does not contribute to the distortion itself. The excitation between the wheel suspension and the body response is quasi-static, this will be verified in the following sections and it will be important for future understanding of this work.

By looking at Figure 2.4 we can observe that the excitation of the wheel is around 12

Hz, and the body modes which are affecting the distortion are between 25 and 60 Hz as a design choice (see Figure 2.3), for sure reasonably away from the wheel excitation. This leads to a frequency gap between 12 and 25 Hz where the assumption of quasi-static response previously assumed is now confirmed, from this point on, a very important simplification will be used from now on: Each time step of the dynamic load history will be approximated to a static load case. The implications of this are huge: not only will optimization procedures not be required, therefore saving time, but will also simplify the complex phenomena, allowing a deeper understanding of the effects of the combination of the forces themselves.

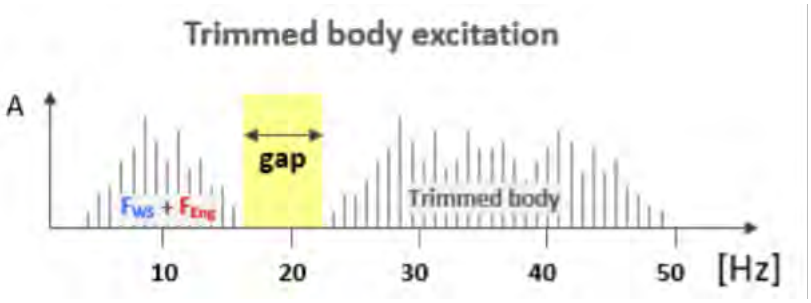

Figure 2.3: Frequency gap between the wheel suspension and trimmed body, indicating a quasi-static response between them.

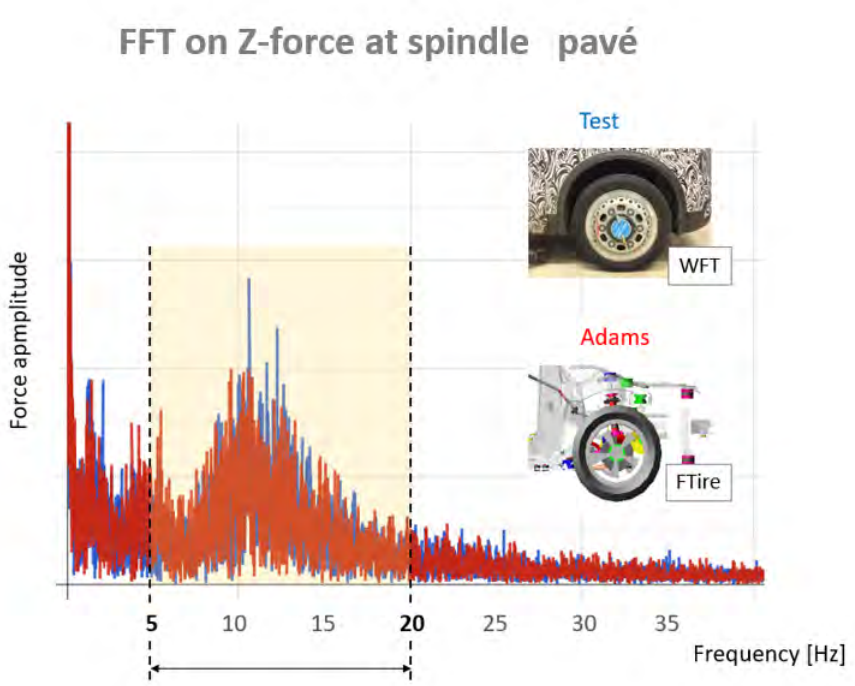

Figure 2.4: FFT (Fast Fourier Transform) on forces on Z-direction (vertical) of the studied vehicle on Belgium pavé. It shows the excitation of the wheels around 12 Hz, which is consistent to the figure 2.3.

2.3. Finite Element Model and Solver (Finite Elements and Multi-body)

Beforehand, a short explanation of a free-free condition is necessary: It is a condition where the structure is free of boundary conditions; therefore, it is able to have rigid body motion in all 6 DOFs in a three-dimensional space, following the same logic, the first 6 natural frequencies should be zero (or very close to it, numerically speaking) when performing a modal analysis.

Thus, there are no boundary conditions being applied in the model. The loads are applied in specific locations; their values are obtained from ADAMS in a Multi-Body Simulation (MBS). The simulation is performed after mapping and tracking the actual road to a virtual track. This is very useful to obtain the data for forces since the trustworthiness of the experimentally measured forces is not high and the difficulties for acquiring forces from experimental data are hard. The Vehicle Dynamics group from CEVT provided the force input file after filtering and post-processing the forces.

For the fully trimmed body, the FEM (finite element model) uses SHELL, SOLID,

CBUSH, and BEAMS elements, containing around 6 million elements and 38 million DOF. A schematic relation between the FEM and the MBS model can be seen in Figure 2.5.

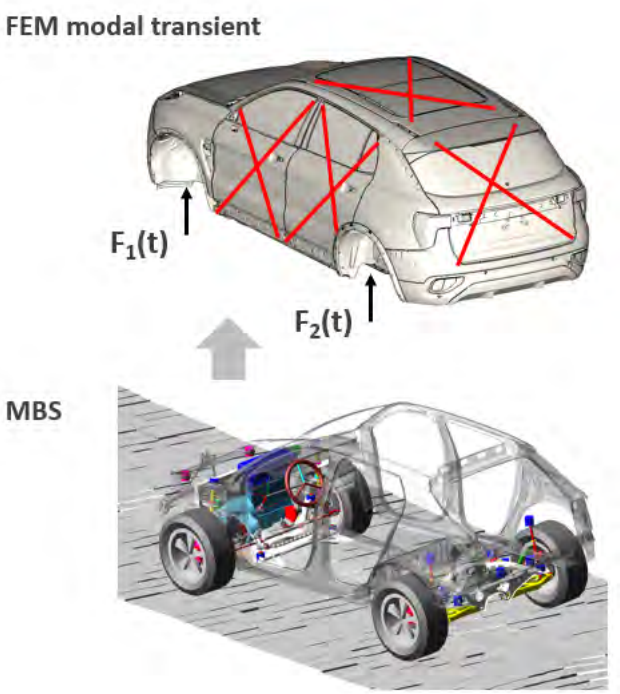

Figure 2.5: Representation of the relation between the FE and MBS models. Note that in the FE model (top) some diagonals are represented in red.

For both static (SOL 101) and modal transient (SOL 112) analyses, simulations are performed in a fully trimmed body of the final version of the vehicle. When using the MSS (multi stethoscope, which is a method to extract information for specific nodes of interest in the post-processing of the analysis), we request the *.pch* file from NASTRAN as output; it will provide us with the displacement of the points of the MSS (desired points) in both the global coordinate system of the vehicle, which is defined in figure 2.6 and the local coordinate system for each diagonal. Note that the figure 2.6 also implicitly states that the X-axis is parallel to the length of the vehicle and Y equal to zero is in the middle of the left and right side of the car. Note that the origin of the Global Coordinate System is in front and below the front of the vehicle. The points associated with the MSS are indeed the nodes of each diagonal on each opening of the vehicle.

A short explanation of the MSS is provided here: It is a finite element model separated directly from the structure, but the desired nodes (associated with the openings of the vehicle) are attached to the nodes in the vehicle model through RBE2 elements. It does not contribute in any way to the deformation or stiffness of the structure but is a very

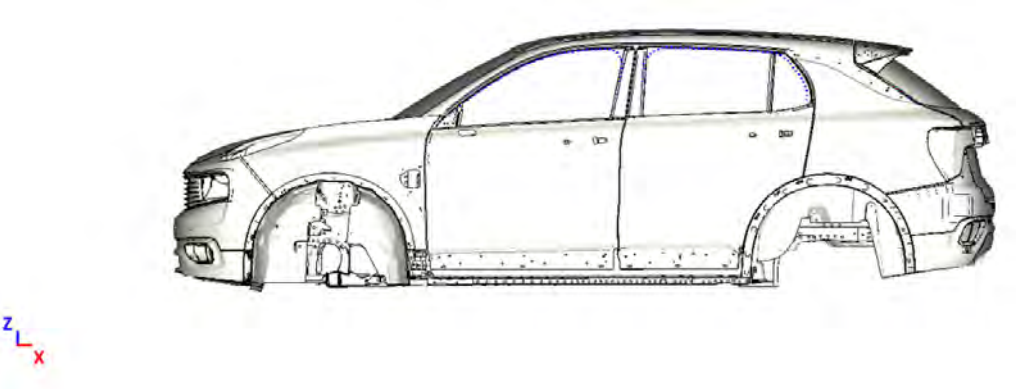

Figure 2.6: Coordinate system of *Lynk & Co 01*. It is located below the vehicle and in front of it, in this way we have only positive values for x and z coordinates, y coordinates can be either negative or positive, since the vehicle is very symmetrical.

efficient way of obtaining the deformations in the desired nodes on both coordinate systems (local and global).

2.4. Distortion calculation

Before understanding a dominant distortion pattern and a distortion pattern, it is preferable to understand what it looks like with the distortion between each opening of the vehicle. We calculate it according to the E-line method [31], where we calculate the difference between each component of the equation in a local coordinate system.

The practical application for the E-line method for the left front door can be seen in figure 2.7 for a given time step, considering both in-plane and out-of-plane distortions *i.e.* dx,dy, and dz. For convenience, we plot them according to the middle point of the opening. For this work, as a convention used by CEVT, the odd node number of the two nodes that define an opening is called the master, and the even one is called the slave. The relative difference between master and slave nodes is always calculated through the E-line method following the convention already specified.

As seen in Figure 2.7 the information concerning D_x,D_y and D_z are condensed in one single point which is associated to a specific time step. This procedure is then repeated for the whole time and history; this will result in a cloud of points.

This cloud resembles an ellipsoid, whose projection in 2D is an ellipse. A simplified version of this ellipse, assuming no out-of-plane distortion; for the sake of easier visualization; can be seen in figure 2.8. Given this strong feeling that the boundaries of such a cloud of points can be approximated to an ellipse, a Principal Component Analysis (PCA) will be able

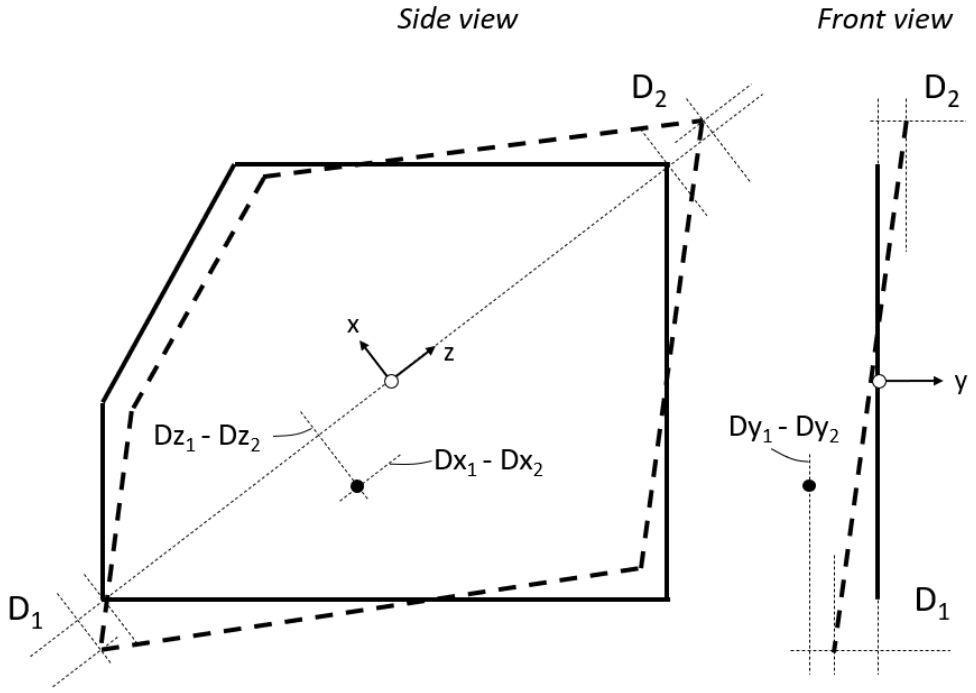

Figure 2.7: Body Opening Distortion. Special attention should be directed to Dx,Dy and Dz. The relative distortion of master and slave nodes (nodes 1 and 2, in this figure) when plotted in reference to the geometrical center of the opening, represents a point in the 3D space.

to provide the principal directions that better describe the distribution of the points in the space (for more details on PCA, check appendix). Once we have determined the principal directions, we can assign a sign for each point, if they are on the positive side of the principal direction, we will call it positive (or +1) and negative (or -1); this becomes especially clear in the figure 2.8 where blue dots are positive and orange dots are negative. In the figure 2.8 after the PCA was applied, the ellipsoid covers all points and the first and second principal directions describe the distribution of the points in space, positive and negative signs are also assigned to the points, a fundamental step for determining a distortion pattern as will be approached in the next section.

This method is also valid and will be strongly applied throughout this work for three-dimensional problems *i.e.* considering out-of-plane distortions as well. Where the ellipse becomes an ellipsoid.

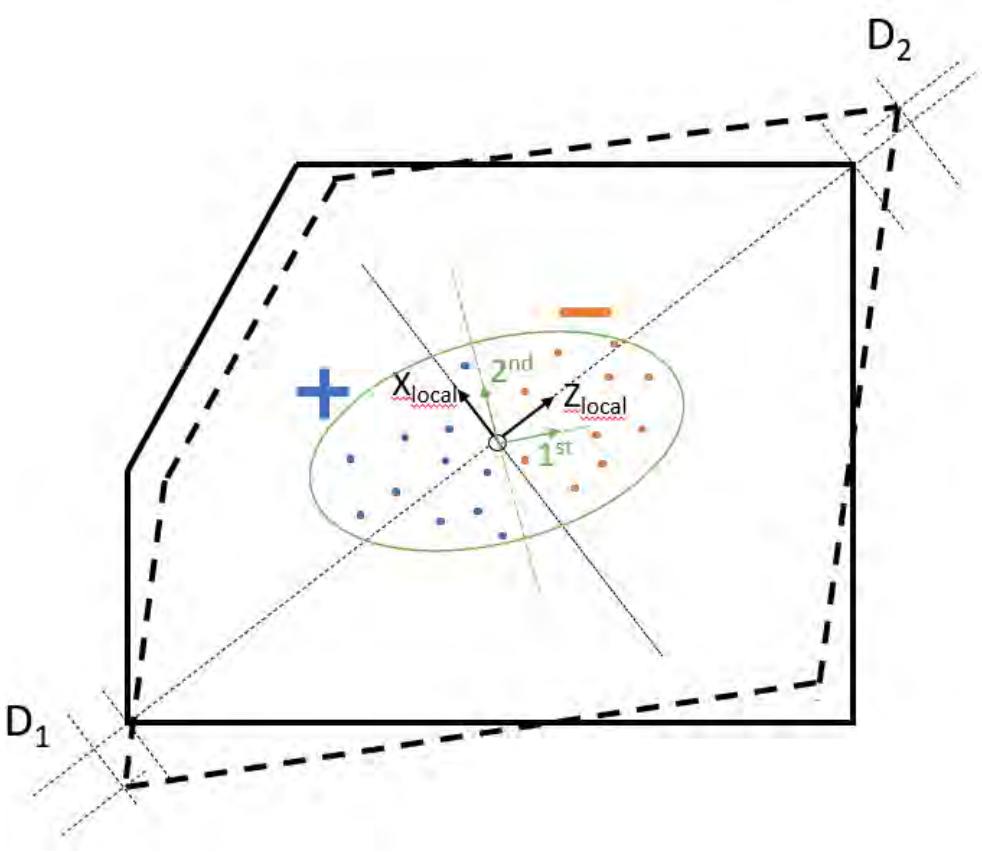

Figure 2.8: Schematic representation of cloud of points simplified to 2 dimensions, for the distortion in the left front door of a conventional vehicle.

2.5. Distortion Pattern (DP) and Dominant Distortion Pattern(DDP)

Once this has been done for one opening, the procedure is repeated for all openings of the vehicle *i.e.* using MSS, meaning that for each time step, every opening has been assigned a sign (+1 or -1). A distortion pattern is simply the combination of +1s and -1s that are obtained from each time step, if we were to consider for example only one of both diagonals that define each opening for the front and rear left doors, as well as the sunroof and the tailgate, we would obtain a distortion pattern as in figure 2.9.

Now it should be obvious that for each time step, a different distortion pattern can be created, since for this work both diagonals for each opening for the four doors, sunroof, rear seat, and tailgate are considered *i.e.* the distortion pattern (DP) will be a vector of dimension 1x14, such as {+1, -1, ..., -1, -1}, which means that unless a very dominant distortion pattern (DDP) is present, many different distortion patterns (DPs) are expected. Very similar distortion patterns could be expected, where 13 terms of the dis-

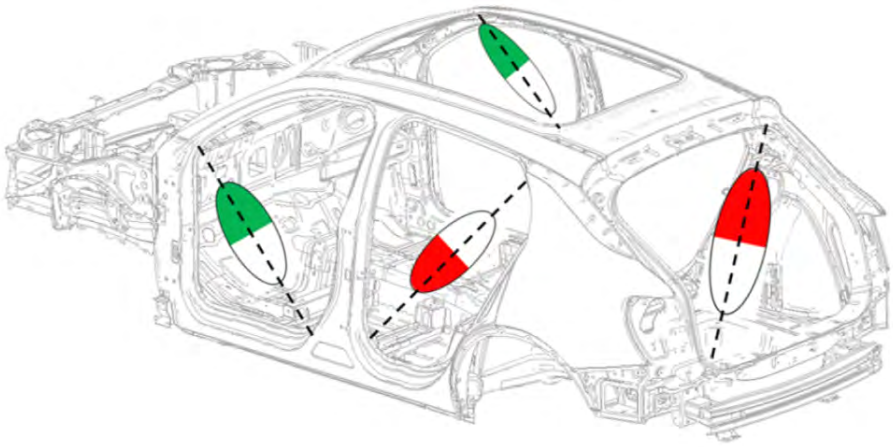

Figure 2.9: Example of Distortion Pattern for some of the openings. Green arrows are representing a positive (+1) value for that diagonal, whereas red arrows are representing a negative value (-1). Time steps that have the same positive and negative values associated with each diagonal have the same distortion pattern.

tortion pattern are equal and only one is different, or almost all of them could be different, mathematically speaking, many scenarios are expected. As implicitly stated, a DDP is a distortion pattern that is dominant with respect to its occurrence along the time history.

2.6. Evaluation of time history

All distortions and forces were measured with a frequency of 500 Hz for 10 seconds, but for the forces, the first 100 data points were ramped from 0 to the values obtained in the MBS, to obtain a smooth curve and guarantee that numerical errors would not occur, thus avoiding non-representative results. Therefore we end up with 4901 points, since the first 100 points are meaningless from an engineering point of view, this however does not alter the results obtained in any way.

After a few seconds of acquisition large amounts of data are obtained, while many time steps of the acquired signals are not adding much information to the problem, thus choosing a smaller sample time, instead of the whole time history will be a clever choice. In fact, using large data makes it computationally costly to use as input for FE models with complex geometries and dozens of force locations *i.e.* where forces are applied.

It is true that the obtained signal is strongly ergotic; in fact, the acquired signals for this work consisted of nearly 2 minutes of acquired data, but due to this characteristic, only the first 10 seconds are used. A few longer and different time samples were employed for

different projects inside CEVT and the results were consistent. This saves some time, but a modal transient analysis would still be required to process such a large amount of time steps.

One simple way of verifying that there are no more significant changes in the data after a given period is to analyze a graph that associates the length of the sample of the time history with the mean overall distortion associated with that time length. Once there is no significant change in the mean value *i.e.* when it reaches a plateau, that sample size should be sufficient, but in any case, a larger value will be chosen for all analyses, since it will provide a safety margin as well as not being excessively more costly from a computational point of view.

2.7. Statistical Evaluation Parameter (SEP)

It is introduced an important parameter: The SEP (Statistical Evaluation Parameter) which varies from 0% to 100%. It is responsible for summarizing the time steps which lead to a certain percentage of the highest values of a parameter of interest. In this work, about the distortions of the vehicle, SEP will be used to sort the percentage of the overall distortion of the vehicle *i.e.* of the sum of the absolute value of the distortions for all 14 openings and for each time step. For the i^{th} time step, the magnitude of the overall distortion of the vehicle can be described by the equation 2.1.

$$D_{total} = \sum_{n=1}^{14} abs(d_n^{i_{th}}) \tag{2.1}$$

The procedure is now explained with further details step-by-step, for a better understanding:

1. For each time step apply equation 2.1 *i.e.* :
   - For each opening calculate the absolute value of the difference between master and slave nodes.
   - Sum the absolute values for all openings, obtaining D_{total}.
2. Sort D_{total} associated with each time step in descending order.
3. Retrieve only the percentage (SEP) of the highest values that you are interested in.

This means that by choosing SEP = p %, you are picking the p % highest overall distortions. The appropriate choice of SEP allows you to focus only on the most critical time

steps.

2.8. Opening Distortion Fingerprint (ODF)

The Opening Distortion Fingerprint presented by Weber *et al.* [32] will be an effective tool for comparing the distortions obtained from the ESL with the distortions from dynamic simulation. In general, the ODF is a distortion analysis in the time domain represented by a two-dimensional bar plot showing the absolute distortion, in millimeters, for each opening, which is shown along the x-axis. The differences between the calculation of the distortion are as follows:

- For the ESL, distortions are calculated according to the E-Line method. A single time step is used, therefore a single value for the distortion for each diagonal is obtained when using SOL 101 with free-free conditions.
- For the dynamic simulation, we are capturing a single frame *i.e.* a time step, and applying the E-Line method. In practice, we are calculating the distortion from the SOL 112 results for all openings and time steps but just retrieving the information from the time step that is interesting to us.

In summary, if we decide that the loads of a given time step are representative of the event as a whole (using SOL 101 with free-free condition), we may compare the results of the ESL that is based on the load case of the aforementioned time step with the dynamic simulation for the same time step (including possible dynamic effects) using SOL 112. In this case, the results should be similar, this will be verified by plotting simultaneously the ODF for both cases for the relevant time steps.

2.9. Vector Participation Plot (VPA)

Once defined the time steps associated with the highest ODs (overall distortions) for the given SEP, we generate a vector participation plot, which will be called VPA, which is a pie chart that shows how often each distortion pattern has occurred during the whole time history; the largest slice of the pie chart will, of course, be the dominant distortion pattern *i.e.* the DDP.

The influence of SEP on the dominance of a single distortion pattern will be analyzed *i.e.* to determine how much more dominant is the DDP in relation to the other possible distortion patterns.

The core question becomes: for the DDP the deformation patterns are the same, is there

a similar relation for the forces that generate the same deformation patterns? *i.e.* Does a DFP (dominant force pattern) exists, in a way that generates the DDP?

Once that has been done, the next step will be to better understand the forces associated with those time steps.

This analysis will be done in two different ways:

1. Force VPA: vector participation plot for the forces considering each force location
2. Moment Analysis: Calculating the relative moment around X (see figure 2.6)

2.10. Force locations and analysis

It is necessary to know the force locations before diving into further analyses: they are symmetric, given the strong symmetry of the vehicle, meaning that if a force is applied in the right top mount in the front of the vehicle, it is also applied in the left top mount in the front as well. The force locations can be seen in figures 2.11 and 2.10.

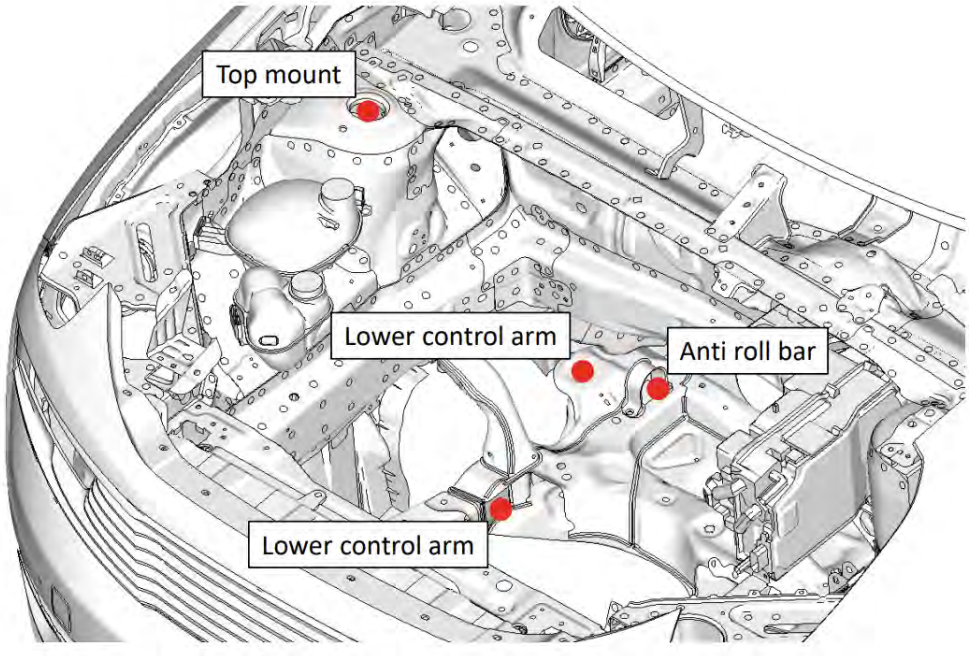

Figure 2.10: Force Locations in the front of the vehicle.

The exact same procedure as described for the PCA for the relative displacement is now performed in the forces for all the force locations. Some differences apply since now we are considering vectors and not a difference of two measurements (displacement of master and slave nodes).

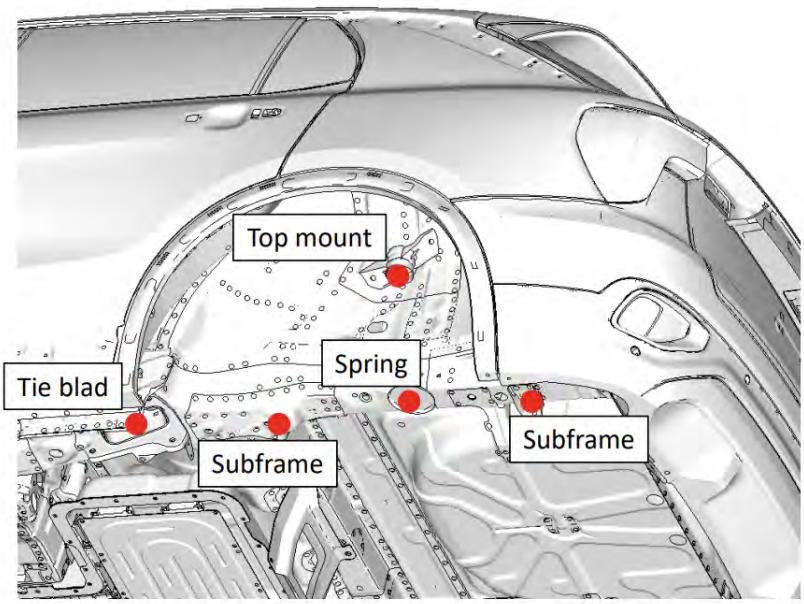

Figure 2.11: Force Locations in the rear of the vehicle.

The first step is to subtract the average value of the load history for all force locations. The reason for doing so is to generate a static offset value in the force output that compensates for constant (or nearly constant) forces such as gravitational and centrifugal forces. After removing the average value of the signal, we proceed to perform the PCA at each force location. The sign for each time step for each location is then determined in the same way as for the distortion pattern *i.e.* Points with positive local values for the principal direction are positive (+1) otherwise they are negative (-1).

After that, we will restrain the number of time steps that we are analyzing by applying a value for SEP and look only at the DDP associated with this value of SEP. In a way, looking at the DDP for a given SEP will be a way of filtering the forces; before looking at them. With the initial hypothesis that DDP is a function of a supposed DPF, we will search for similarities of the forces given the similarity of the distortions. It is still important to emphasize that the SEP is applied in the distortions, in this way, high ODs and the DDP are responsible for filtering which forces will be further analyzed.

In addition to the Force VPA, a Moment Analysis will be performed. Analyzing the moment is a reasonable approach, given that the torsion is relevant. Looking at figures 2.12 and 2.13 which represent the forces in the yz plane for the front and rear of the vehicle, respectively, there is a good indication of the forces generating a moment around X in respect to the center of gravity of the vehicle. Forces in blue are considered positive, while those in red are considered negative. The dot in the center of the figure is the center

of gravity (COG). Forces are shown in Newton and are drawn on a scale of 5N for each 1 mm, which is the unit for the position of the forces in the y and z axis. The sole purpose of this representation is to obtain an initial understanding of the relation between the forces and the torsion of the structure.

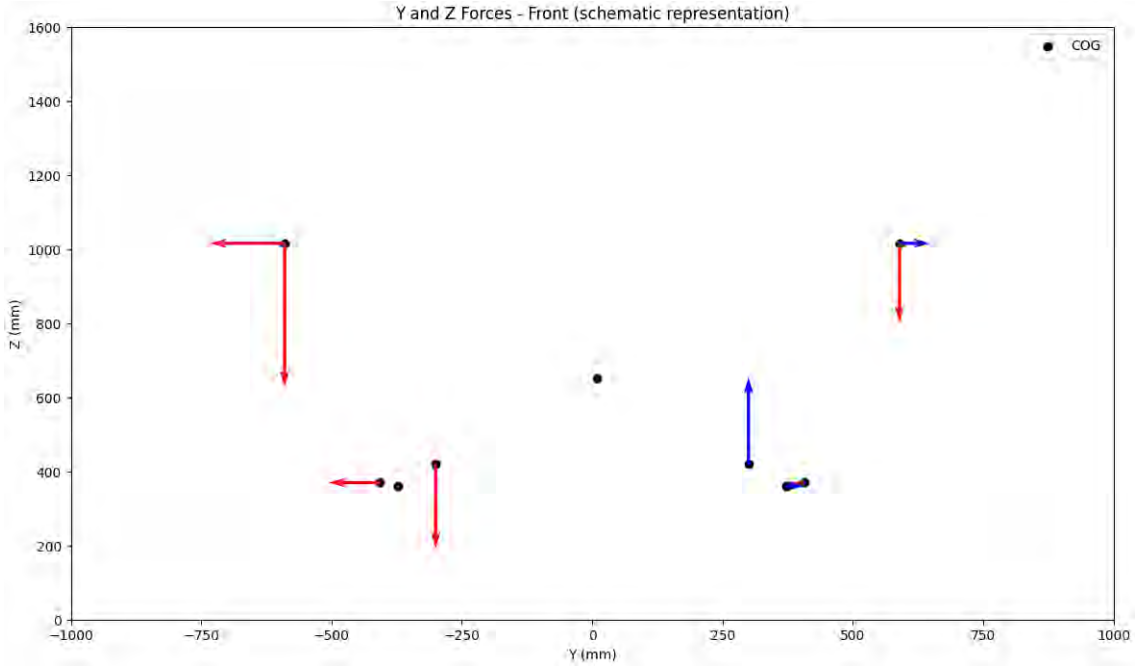

Figure 2.12: Forces in the front of the vehicle for a given time step. Red vectors represents negative forces (in respect to the coordinate system) and blue vectors represents positive forces. It can be inferred that those forces are generating a strong moment in the x direction.

2.10.1. Force VPA

- Considering the force patterns considering only one vector with all forces from both the front and rear of the vehicle at the same time.
- Generating two force patterns, one for only the forces in the front and another one for only the forces in the rear of the vehicle. Basically, splitting the vector obtained in the aforementioned alternative into front and rear is a very reasonable approach as will be shown in different aspects throughout this work.

2.10.2. Moment Analysis

The relative moment is calculated as the difference between the front and rear of the vehicle calculated with respect to the center of gravity (COG), which is also close to

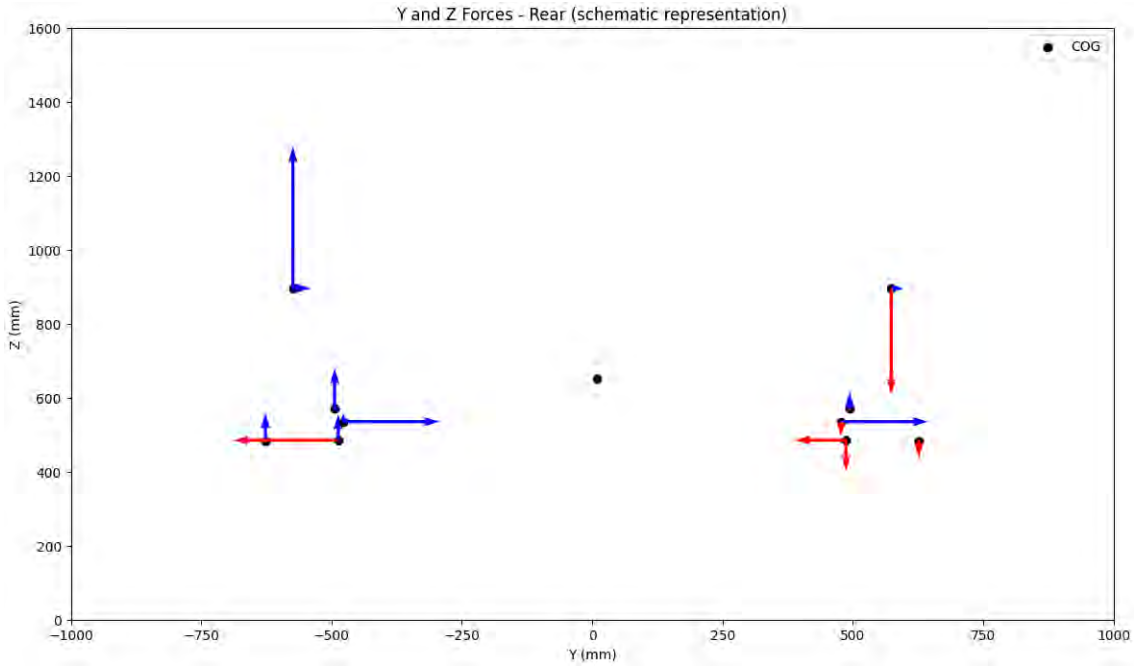

Figure 2.13: Forces in the rear of the vehicle for a given time step. In the sme way, red vectors represents negative forces (in respect to the coordinate system) and blue vectors represents positive forces. It can be inferred that those forces are generating a strong moment in the x direction.

the center of rotation for all the time steps studied. The motivation for calculating the relative moment is that when analyzing the dominant distortion patterns through the optimization procedure from previous studies inside CEVT, for the same vehicle, it was confirmed that the dominant behavior of the structure was a pure torsion around X.

For each time step, the moment in front and rear of the vehicle are calculated following the equations 2.2 and 2.3, respectively.

$$M_{front} = \sum_{i=1}^{n} F_y^i \cdot z^i + F_z^i \cdot y^i \tag{2.2}$$

$$M_{rear} = \sum_{j=1}^{m} F_y^j \cdot z^j + F_z^i \cdot y^j \tag{2.3}$$

Where F_y and F_z are the components of the forces in the y and z directions, respectively, y and z are the distances in the y and z directions, respectively, between the force location and the COG of the vehicle, the superscripts i and j refer to the forces in the front and rear of the vehicle, respectively.

For each time step, the relative moment M_{diff} is then calculated as described in equation 2.4.

$$M_{diff} = M_{front} - M_{rear} \tag{2.4}$$

2.10.3. Moment Categories

4 categories will be used to define the combination of M_{front} and M_{rear}, the reason for doing so is to understand if there is a clear relation between the moment in the front and in the rear *e.g.* both of them should have an opposite sign and high intensity, to be able to generate the DDP with high overall distortion. The categories are as follows; note that there are two possible ways of obtaining category 1 which is essentially opposite moments with non-negligible amplitudes, the same applies to category 4 where both of the moments are high with respect to the other one but they have the same sign. Figure 2.14 schematically represents the moment categories. Note that the moments calculated in this section are exclusively due to the obtained forces and not the inertia of the vehicle.

- Category 1: $|M_{front}| > |M_{rear}|$ with $|M_{rear}| > 20\%|M_{front}|$
- Category 1:$|M_{rear}| > |M_{front}|$ with $|M_{front}| > 20\%|M_{rear}|$
- Category 2: $|M_{rear}| > |M_{front}|$ with $|M_{front}| < 20\%|M_{rear}|$
- Category 3: $|M_{front}| > |M_{rear}|$ with $|M_{rear}| < 20\%|M_{front}|$
- Category 4: $|M_{front}| > |M_{rear}|$ with $|M_{front}| > 20\%|M_{rear}|$
- Category 4: $|M_{rear}| > |M_{front}|$ with $|M_{rear}| > 20\%|M_{front}|$

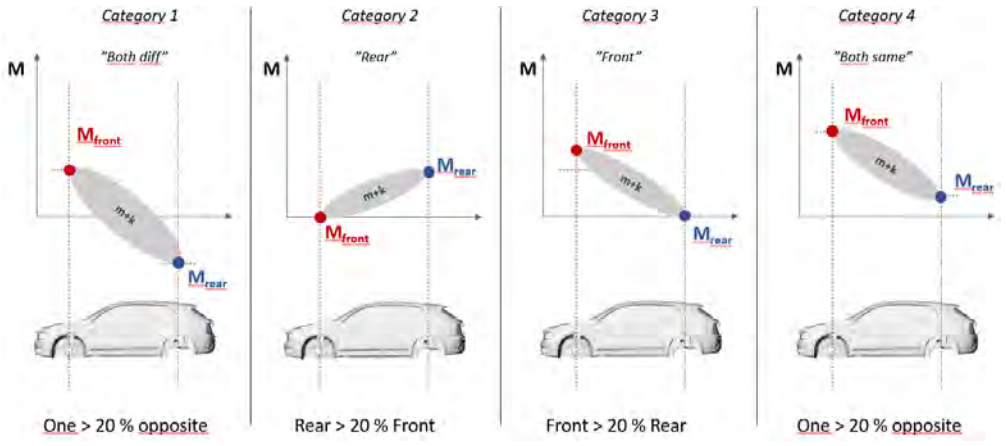

Figure 2.14: Schematic representation of the moment categories.

2.11. ESL

As already mentioned, the assumption of quasi-static response is the principle to simplify obtaining an ESL. This can be verified by comparing the ODF for a dynamic run for a given time step with the same loads at that specific time but running a linear static analysis (SOL 101). If our assumption is true, both ODFs should be very similar

In the state-of-the-art chapter, in figure 1.3, it was possible to observe a similarity of the ODFs. However, a single linear static analysis was compared with loads obtained through optimization, with an average of several (in that case for the chosen SEP, 1500) time steps as the target of the optimization problem. Not only that, but the force locations were reduced only to the 4 top mounts of the vehicle, it has already been shown and will be further demonstrated that this simplification, and therefore that result, is not realistic from a force analysis perspective.

The implicit assumption of this work is that the load case from a specific time step will be able to reasonably represent the global behavior of the structure, as well as a critical scenario *e.g.* high OD. Therefore, being an advantage in relation to the state-of-the-art, since it will not require an optimization procedure. The optimization would force the existence of loads that would represent the real phenomenon, while we could obtain this by looking at a representative time step. This will be a more efficient and faster method.

3 | Results

3.1. Highest Overall Distortions

Not all time steps are relevant so we will focus on the highest Overall Distortions (ODs). The motivation, as already explained, consists of looking at time steps with high OD since they represent the most critical cases. This means that a low value of SEP (*e.g.* 10%) leads to high ODs, this concept will be extensively used in this work and therefore it is recommended to keep this in mind.

Just by looking at the overall distortions of each time step chronologically, we would capture an image similar to Figure 3.1. If we were to rank the time steps from higher to lower with respect to their overall distortions and look at a given value of SEP *e.g.* 10%, we would be looking at figure 3.2.

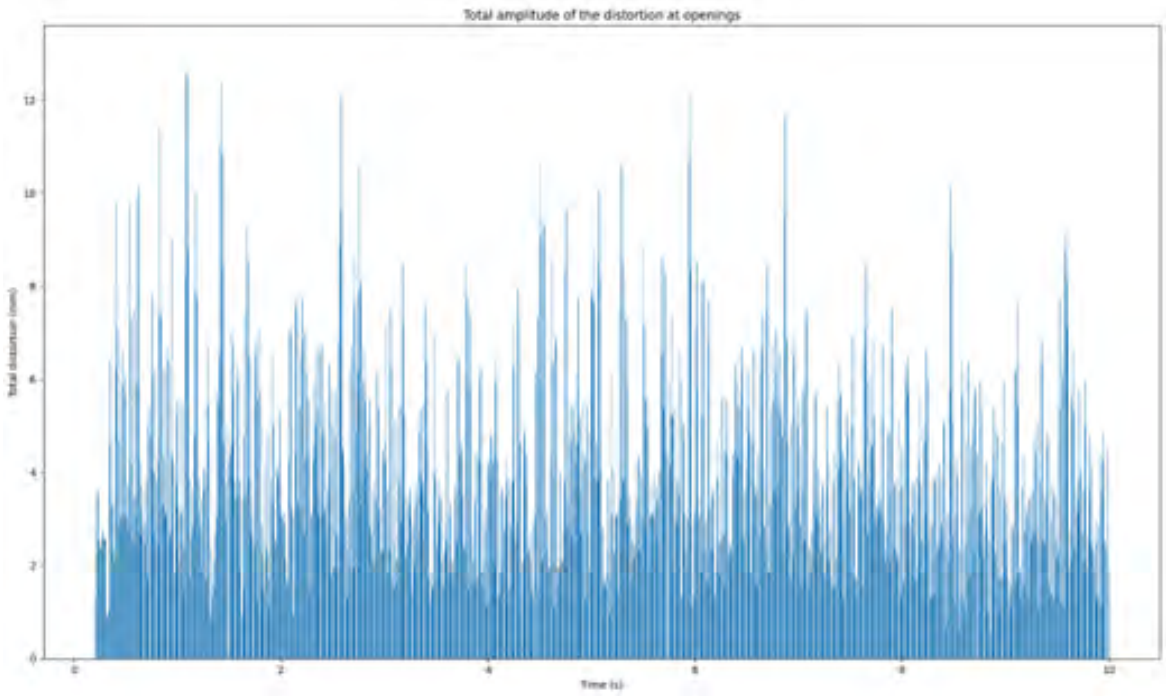

Figure 3.1: Overall Distortion considering the whole time history. For each time step, it is plotted the overall distortion of the openings for that time step.

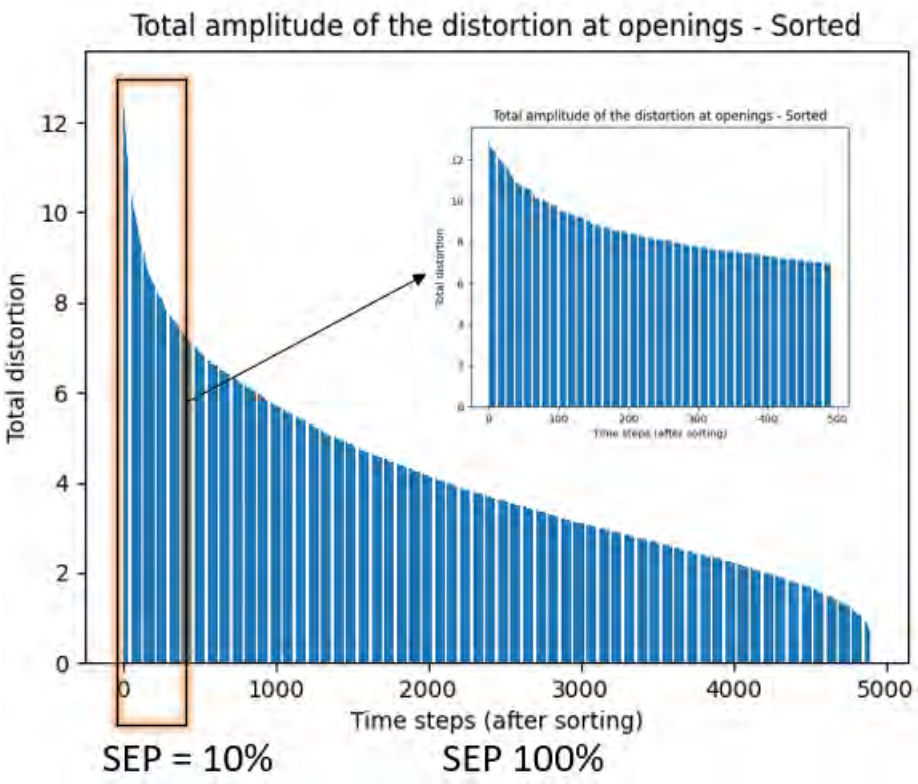

Figure 3.2: Overall Distortion after ranking the time steps with the highest ODs. The order of the time steps is no longer present, but now focus can be given to the time steps where the overall distortion is higher. It is also shown the 10% highest overall distortions.

3.2. Distortion Analysis

After understanding what SEP is really doing with the time history, from the last section we can focus on what this is doing with the distortion plot in 3D for one of the openings, in this case, one of the diagonals in the tailgate. Just by plotting the distortions for the entire time history before applying Principal Component Analysis (PCA) *i.e.* before defining what a positive or negative point is, we capture well-distributed cloud points in an ellipsoidal shape (approximately), as seen in Figure 3.3.

The distribution of points clearly has a preferential direction (as well as second and third preferable ones), the PCA analysis will define the principal directions, as explained in the methodology chapter, points will be assigned a positive or negative value. In figure 3.4 we have the results of the classification procedure (positive or negative) of the figure 3.3.

Then, for each time step, a sequence (a vector) of positive and negative values is created for each diagonal, defining a distortion pattern. Plotting 3.4 for all diagonals at the same time in their respective locations in the vehicle (scaling the distortions by a factor of 100,

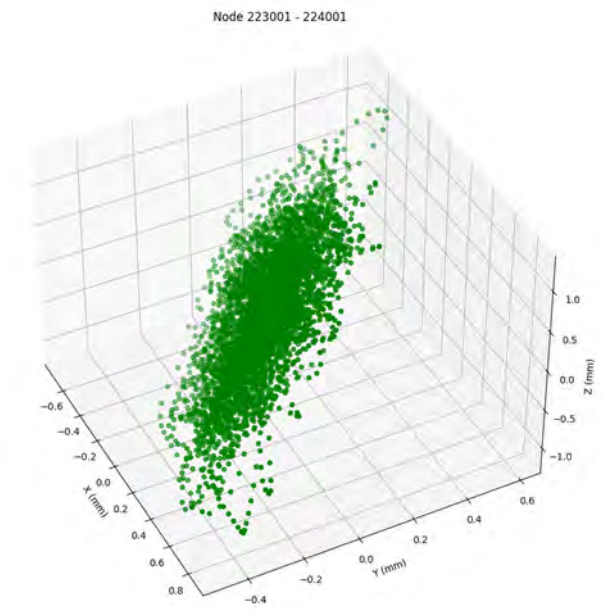

Figure 3.3: Distortion for the whole time history, before PCA. The relative distortion is plotted in 3D in reference to the geometrical center of the diagonal. The cloud of points similar to an ellipsoid is clear, but no more information can be inferred.

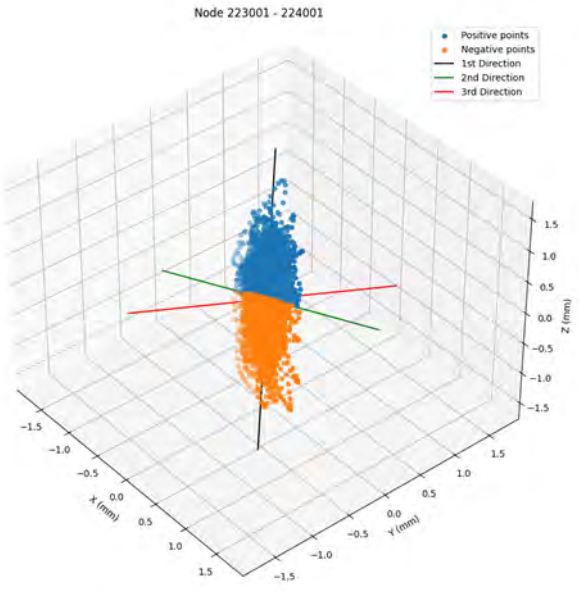

Figure 3.4: Distortion and classification of points after PCA. Differently then figure 3.3 the same points can be reinterpreted based on their distribution in space, the second and third principal direction form a plane that serves as criteria to split two sets of points, one of them attributed a positive value (+1) and the other as negative (-1).

to be able to be visible) leads us to figure 3.5. The big cross in the middle is the sunroof, on its right, we have the right doors, on its left, we have the left doors, right below it we have the rear set and tailgate, respectively. For all diagonals the plot observed in figure 3.4 is also present here, to provide a deeper understanding of the geometry of the problem.

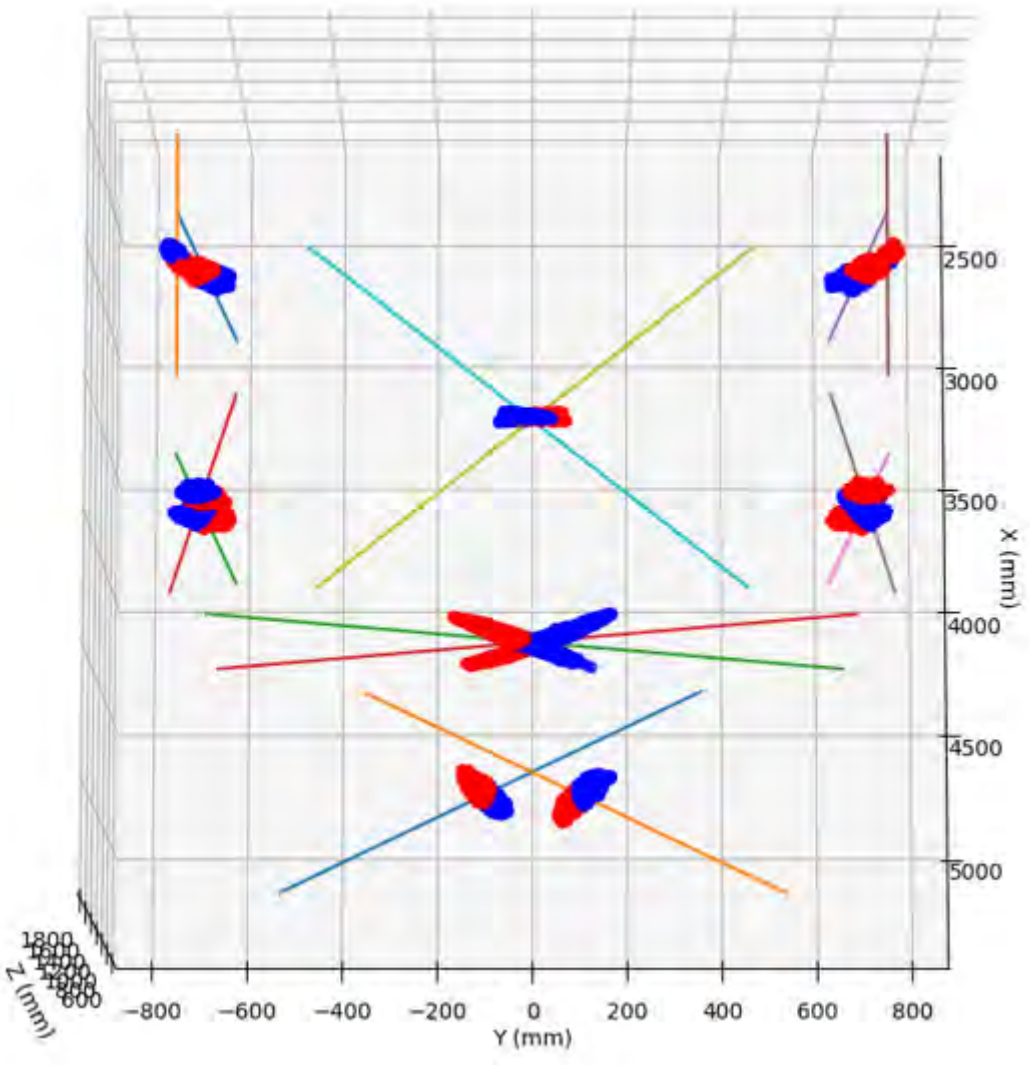

Figure 3.5: Distortions at all openings in the vehicle, distortions scaled by a factor of 100. On the top of the image we have the front of the vehihcle, on the left we have the left doors, on the right the right doors, the big cross in the middle of the image represents both diagonals in the sunroof, right below it we have the two diagonals of the rear seat and below it the tailgate with its diagonals.

3.3. VPA and DDP

A comparison is performed between the vector participation plot (VPA) for the distortion considering different SEPs. Figure 3.6 represents all possible distortion patterns and how often they appeared. The dominance of one distortion pattern with 53.7% of all time steps is notorious, even when analyzing all time steps this pattern is already considerable, this will be emphasized when analyzing only the highest overall distortions in the next section.

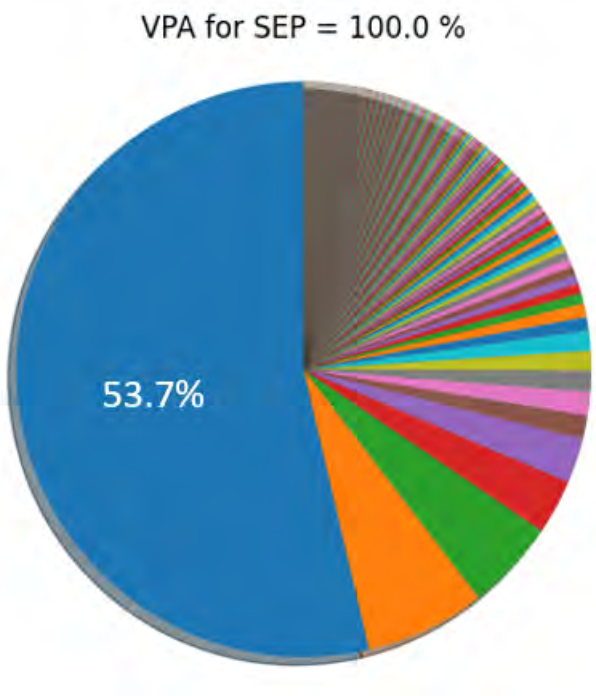

Figure 3.6: VPA of the distortion for the whole time history. It is notable the dominance of one distortion pattern represented by the largest portion of the pie chart, in blue, with 53.7% of all time steps.

Two things stand out from this result:

- Although there were 8192 possible mathematical possibilities ($\frac{2^{14}}{2}$), only 342 patterns occurred throughout the 4901 time steps.
- One distortion pattern is clearly dominant, even when considering the whole time history, more than half of the time steps are associated with the same distortion pattern (even though there are 342 patterns that occurred).

Given the symmetry of the problem, we consider that if a distortion pattern is the negative version of another distortion pattern, they are equivalent to each other; therefore, half of

the possible scenarios are possible: 2^{13} instead of 2^{14}.

3.4. SEP influence

Still in the same line of thought as in the VPA and DDP sections. The dominance of the dominant distortion pattern becomes even more pronounced when we decrease SEP, therefore looking at the highest ODs, figure 3.7 clearly demonstrates how the Dominant Distortion Pattern (DDP) increases its dominance when SEP decreases *i.e.* by looking at the cases with the highest ODs. In fact, for SEP = 10%, only 3 patterns occurred, showing absolute dominance of the DDP. From now on, low values of SEP, such as 5 or 10%, will be the main focus of this work, given the dominance of the DDP for such values of SEP, leading to a more clear relation of the DDP with a possible ESL.

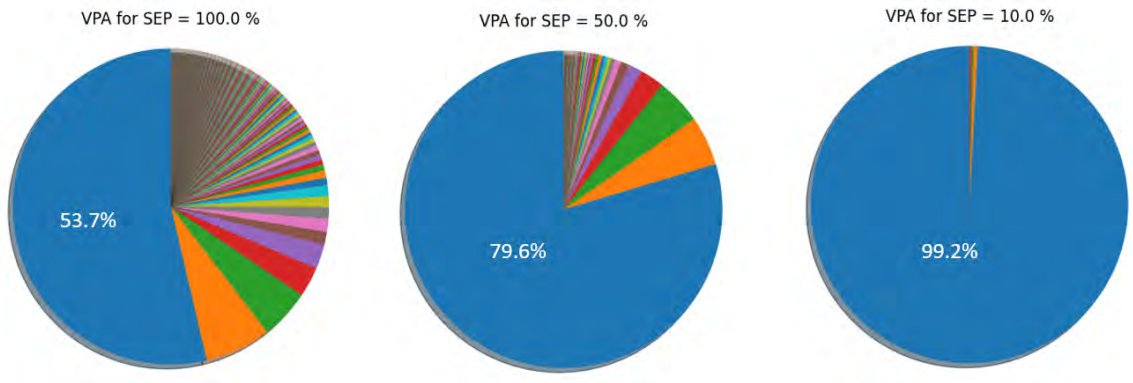

Figure 3.7: VPA of the distortion for different SEPs. Showing an increase in the dominance of the DDP.

Figure 3.4 is associated with a SEP of 100%, and this picture can change a lot if we look at different values of SEP, not only because we are looking at fewer points, but because by looking at higher ODs we disregard the points closer to the center of the image *i.e.* small distortions.

This can be verified by looking at figure 3.8, which exemplifies that time steps with small distortions are not relevant when we analyze the highest overall distortions. It is true that we are analyzing only one diagonal in this figure, but it is also reasonable that in order to have a high OD it is necessary that each opening be reasonably high. This does not necessarily imply that for a given SEP, an opening cannot contain a time step that is considerably smaller than the average *e.g.* see a smaller point inside the nearly circular figure formed in Figure 3.8. As long as the sum of all the distortions for a given time step is sufficiently higher than a certain percentage of others, small distortions can be found at any diagonal if the overall(global) distortion is high enough.

In the end, since the decrease of SEP leads to higher ODs, it is expected as well that for each diagonal we are focusing our attentions to relative displacements that are reasonably large, therefore far away from the center of the plot.

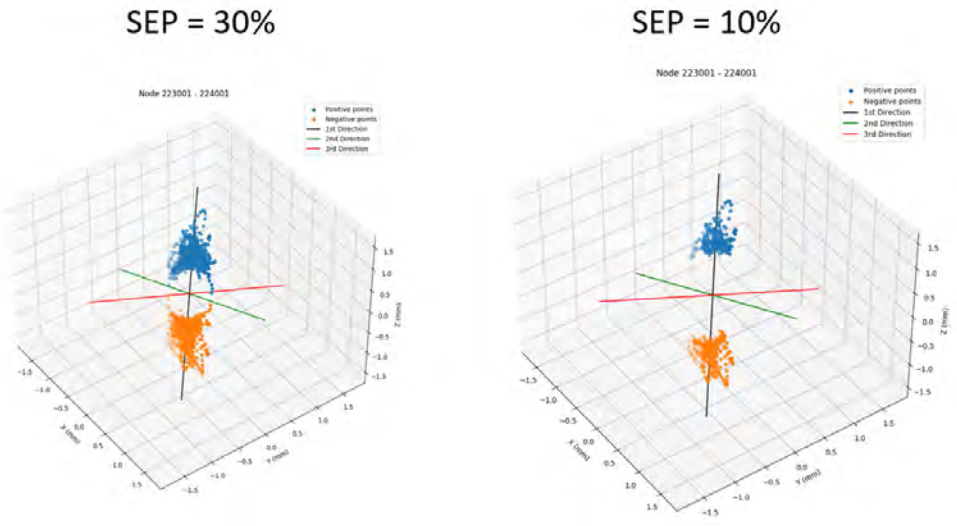

Figure 3.8: Influence of SEP in the distortion, vanishing with the points close to the origin of the pot.

If we compare the plots in figure 3.8 we will see that the hole appeared in the center of the cloud points (in the left figure) and it changes to a situation where only the points in the extremity of the cloud are relevant *i.e.* those that are associated with high distortions.

3.5. Opening Distortion Fingerprint (ODF)

We will now focus on SEP set at 10% as already mentioned in this work. Three time steps will be studied, the ones with the highest overall distortion. The forces for each of those time steps will be used as an ESL, and the distortions in each diagonal will then be used to compare with its equivalent time step in the dynamic simulation, and the goal will be to confirm the hypothesis of quasi-static response by a different method, instead of the FFT presented in the methodology chapter. A comparison of the ODFs of the three time steps will also be made.

The three time steps with the highest overall distortions were 1.096 s, 1.428 s, and 2.584 s, respectively. Important to note that consecutive time steps are separated by 0.002 s and therefore are not considered, only the time steps with the highest overall distortions for consecutive time steps are chosen.

The procedure, as explained in the methodology, will consist in performing a static analysis

with the dynamic loads retrieved from the time steps related with the time 1.096 s, 1.428 s, and 2.584 s (using them as ESLs). Since we have already ran the dynamic simulation we will retrieve the relative displacement between the nodes of the diagonal and compare the similarity of the values obtained between the static and dynamic simulations, this plot is what we call ODF.

If the results between dynamic and static simulations are similar, this means that indeed the quasi static response between the wheel and the body is indeed valid and our simplification that implies that no optimization will be required to obtain an ESL is true, although it will not explain which time steps we should focus on, this will approached in section 3.7. The results for the aforementioned time steps can be seen in figures 3.9, 3.10, and 3.11.

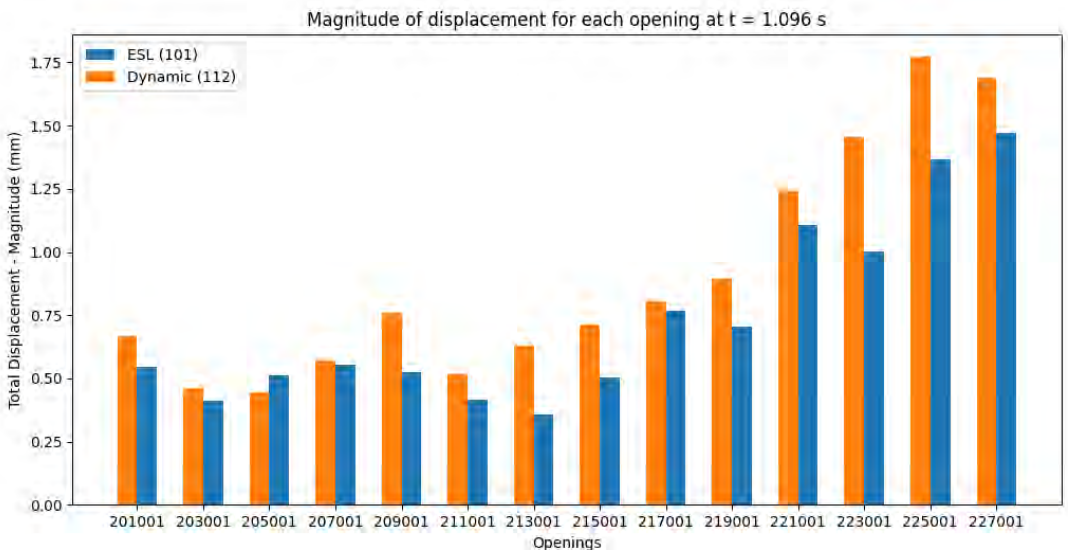

Figure 3.9: ODF for t=1.096 s.

We can see the similarity of the results when comparing the ESLs and the dynamic results for that specific time step; on the other hand, for t = 1.096s we see a reasonably big difference for some of the diagonals. The similarity of the shapes of the ODF, not necessarily the magnitude of the distortion, is also relevant.

What is done next is to compare the relative distortions for all openings for the 5 time steps with the highest ODs when used as ESLs with the highest OD from the whole dynamic time history. Results can be seen in figure 3.12.

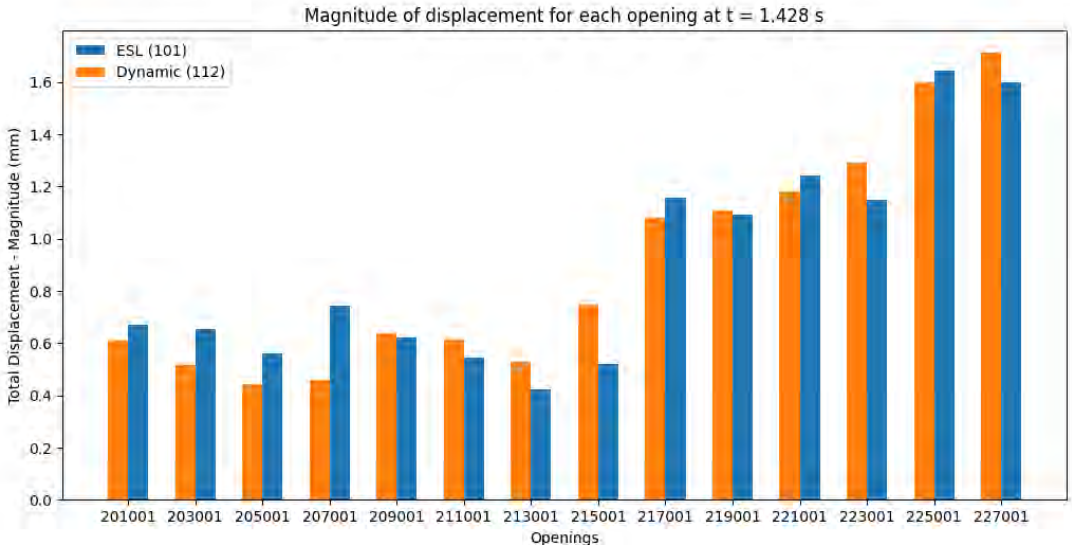

Figure 3.10: ODF for t=1.428 s.

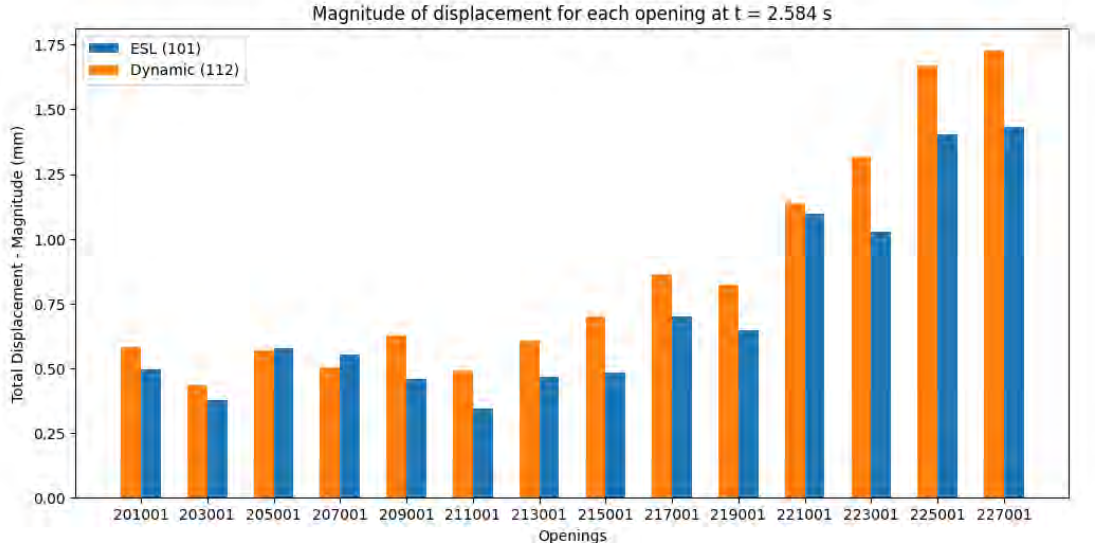

Figure 3.11: ODF for t=2.584 s.

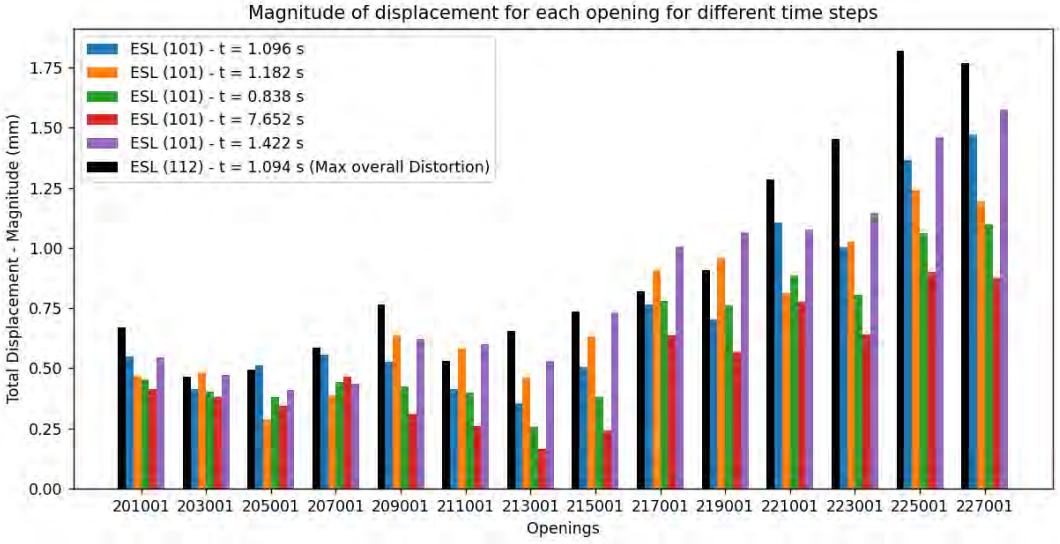

Figure 3.12: ODF comparison among 5 ESLs with the highest OD and the highest OD from the dynamic simulation considering the whole time history.

3.6. Force Analysis

3.6.1. Force VPA

Similarly to figure 3.4, the positive and negative values of a given force location for all time steps can be seen at figure 3.13. Plotting all of the forces in the vehicle at the same time is represented in figure 3.14. The plane generated by the second and third principal directions is the reference to separate the two sets of points, the positive and negative ones.

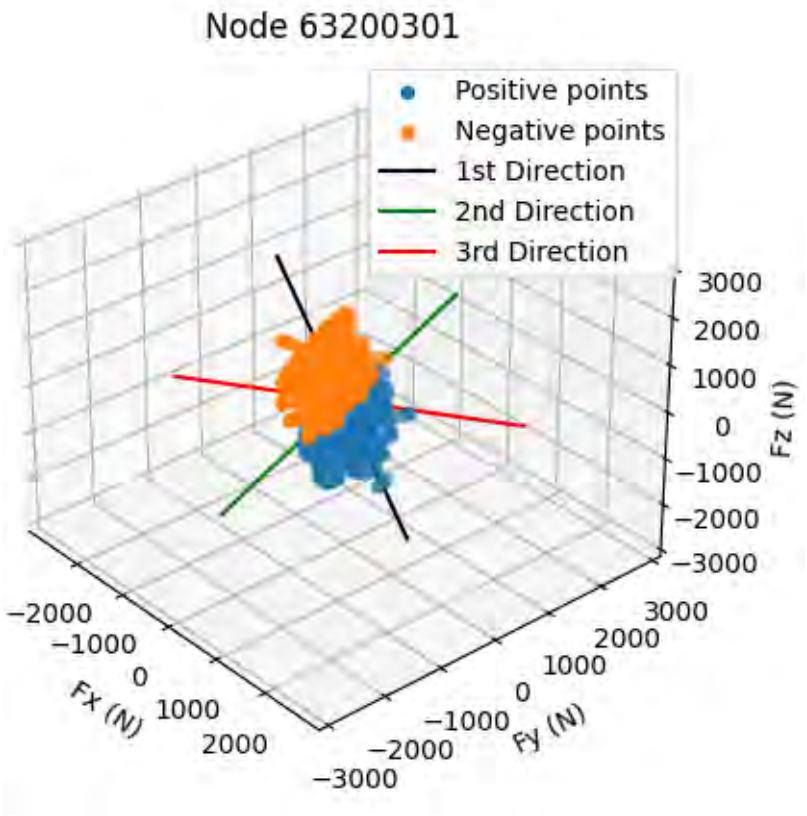

Figure 3.13: Forces after removing average value and applying PCA. The process of assigning a positive or negative value for each point is the same as for the relative distortions, points in different side of the plane generated by the second and third principal directions are assigned opposite values.

No force location is representing a small magnitude (although forces are divided by a factor of 200), meaning that in relation to other forces, all of them should be considered, and it is also pointed out the high magnitude of lateral forces, comparable even with the magnitude of the forces on the top mounts.

Based on the same procedure, the possible force patterns and how often they appeared

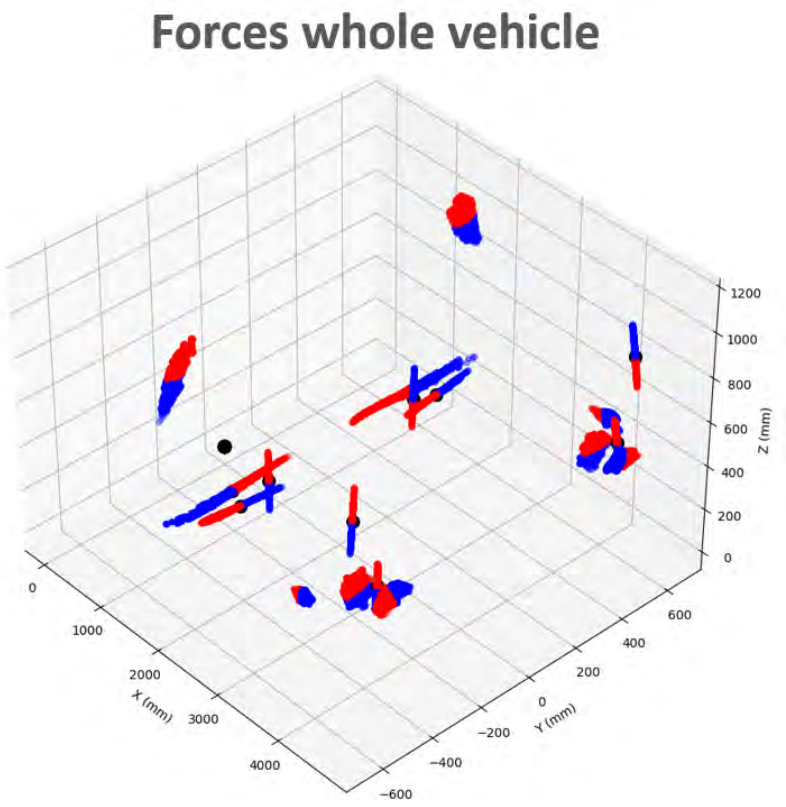

Figure 3.14: All clouds of points representing the forces in their respective location with the origin of the coordinate system the same as presented in the figure 2.6. It can be noticed high lateral forces, specially in the front of the vehicle. The forces on the top mounts in the front are also not entirely vertical.

are compiled in a pie chart, the Force VPA and results can be seen in Figure 3.15.

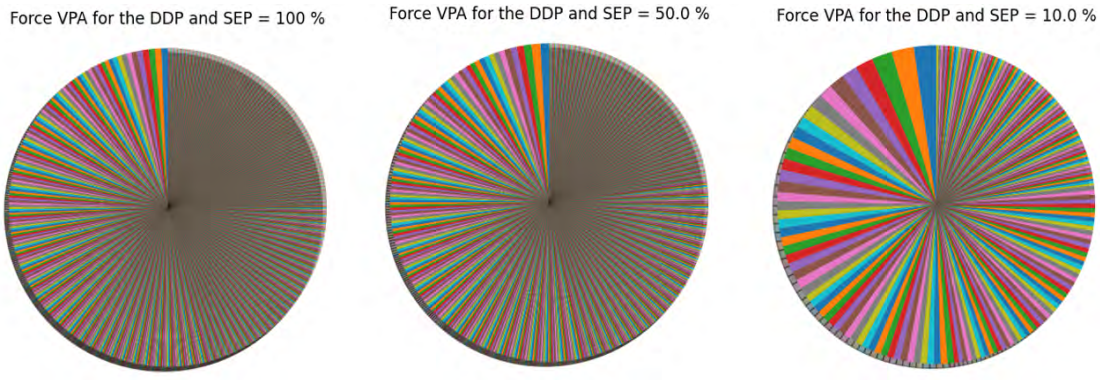

Figure 3.15: Force VPA and influence of SEP. No clear influence of SEP is present, there is no clear dominance of any force pattern.

SEP influence is not clear in figure 3.15, although there is an increase in the slice size of most force patterns with the decrease of SEP, the number of different patterns is also

decreasing. There is no dominant force pattern. The logical conclusion is that the force pattern is not a valid tool to understand how forces generate the same DDP. In fact, the forces generating the same Dominant Distortion Pattern can greatly vary not only in magnitude but also in direction.

A comparison between the first three most relevant Force Patterns (DFP) is performed, the aim being to observe if the forces shared any similarities, within each Force Pattern (FP), as seen in figures 3.16,3.17 and 3.18. The X-axis represents the number associated with the nodes of the force locations and the Y-axis is the magnitude of the forces in Newtons(N). Note that the sign of the plot *i.e.* positive or negative forces are associated with the sign obtained from the PCA. This means that a negative force in this graph is merely a force that has a negative sign inherited from the PCA. Each column for a given force location represents the magnitude of the force (with the assigned sign) for a given time step within that force pattern.

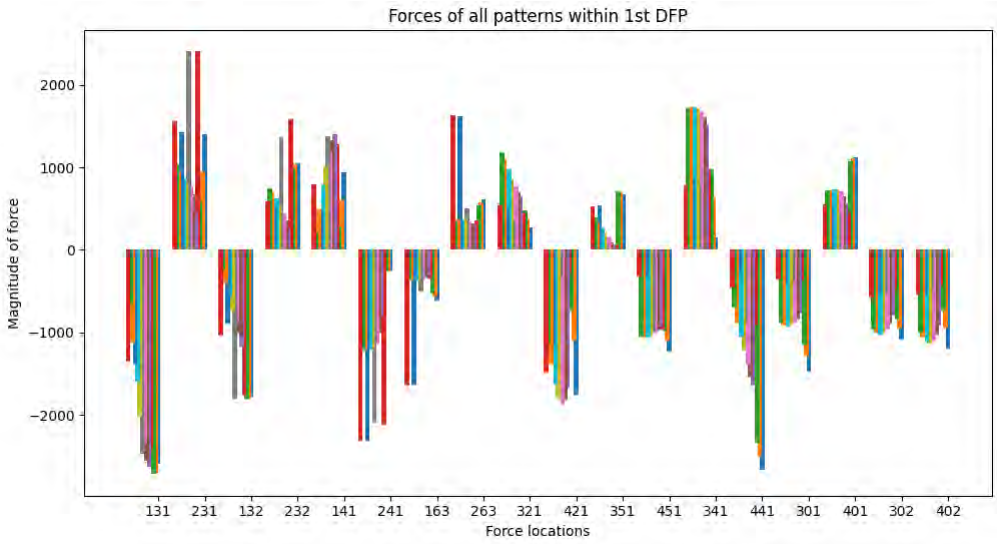

Figure 3.16: First Dominant Force Pattern. No clear proportionality between different force patterns(comparison between bars with the same colors).

No significant insight was obtained from figures 3.16,3.17 and 3.18, and the assumption of proportionality of the forces between time steps belonging to the same force pattern *i.e.* a high correlation was not verified. Therefore, analyzing force patterns to predict the DDP will not be a valid approach.

The comparison made on figure 3.18, on the other hand is not so significant, since there are only 4 time steps associated with this force pattern, yet it it is the third dominant force pattern, meaning that similar results were obtained for the fourth, fifth, and others force patterns. This was verified, but was not shown here due to lack of significant contribution

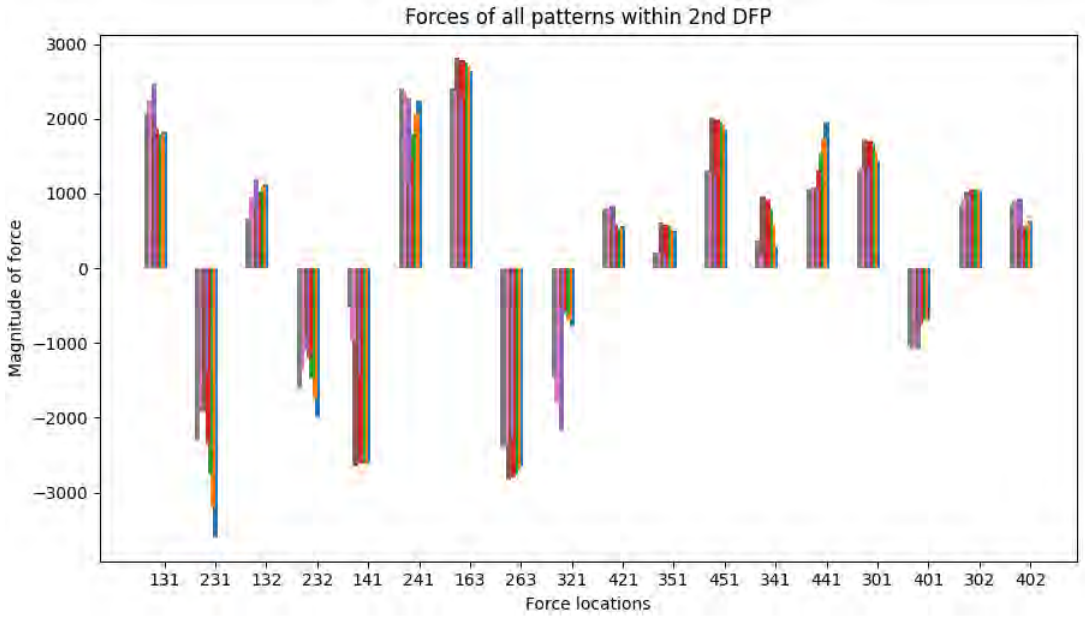

Figure 3.17: Second Dominant Force Pattern. No clear proportionality between different force patterns(comparison between bars with the same colors).

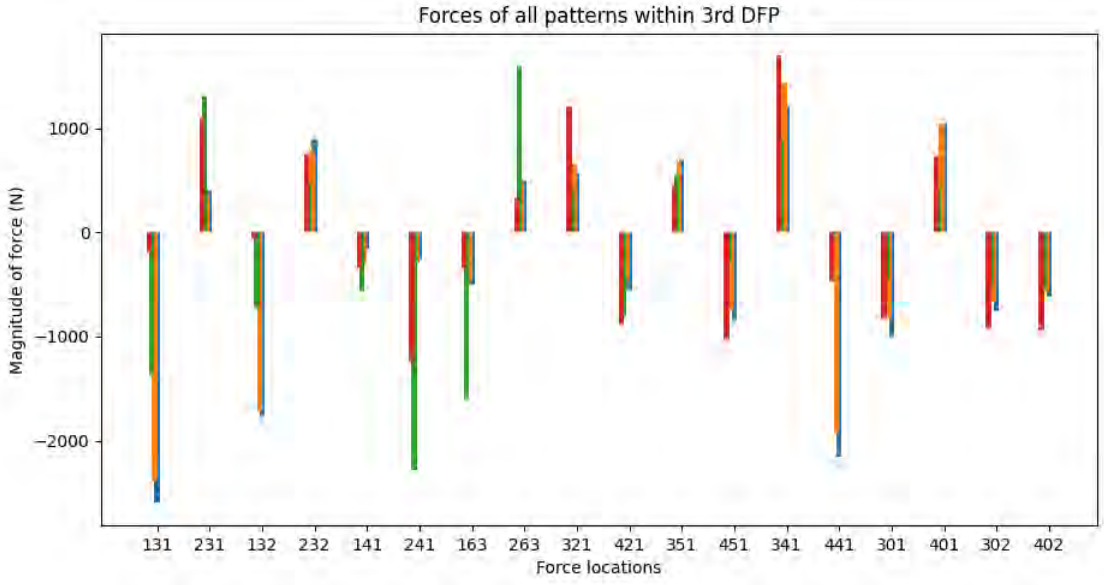

Figure 3.18: Third Dominant Force Pattern. No clear proportionality between different force patterns(comparison between bars with the same colors).

for the work.

Analyzing all of the force locations has proven not to give too much insight to better correlate the forces and the distortions in the openings; therefore, analyzing separately the forces in the front and in the rear of the vehicle will be presented. Splitting the figure

3.14 into two figures (3.19 and 3.20) and then performing the PCA and describing the force patterns separately will provide more information about the vehicle. The force VPA for this scenario is shown in Figure 3.21.

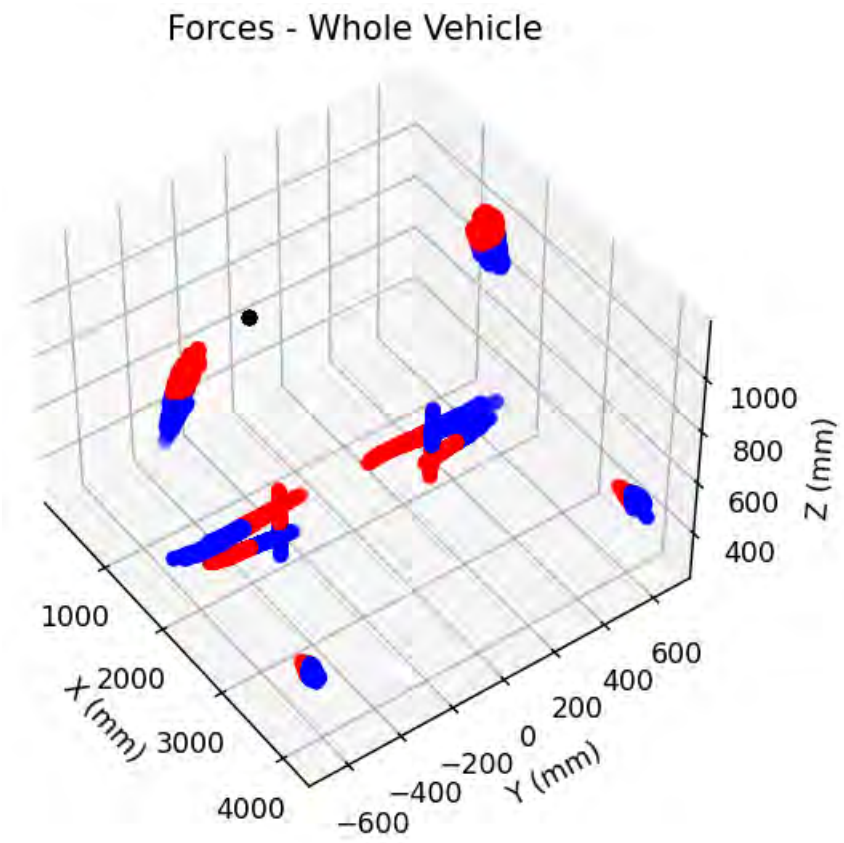

Figure 3.19: A zoomed view of figure 3.14 but focused only on the force locations in the front of the vehicle.

Figure 3.21 shows a big decrease in the number of possible force patterns, however, this can be explained due to the fact that instead of analyzing 18 force locations (2^{17} mathematically possible combinations) we are analyzing two possible force patterns of 10 forces in the front and 8 forces in the rear of the vehicle. It should also be pointed out that the rear contains less forces than thee front, leading to a smaller amount of possibilities and consequently larger slice of the more dominant force pattern on the rear.

One aspect of this investigation is that the time steps associated with the largest slices of the pie charts of figure 3.21 have no correlation, indeed the front and the rear behavior of the vehicle are completely separated behaviors.

The difference between the biggest slices between the front and rear can make use of the same argument. Therefore, analyzing the force patterns, even when there are slightly

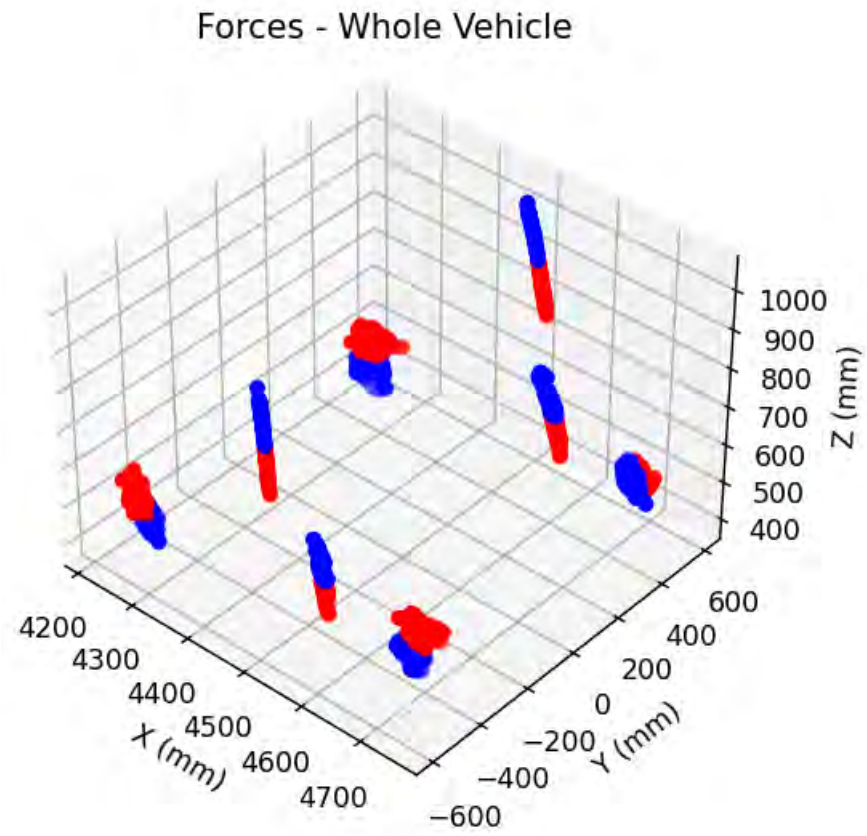

Figure 3.20: A zoomed view of figure 3.14 but focused only on the force locations in the rear of the vehicle.

fewer combinations (even with a small SEP), did not lead to a clear understanding of the relation between forces and the dominant distortion pattern either.

In fact, even the dominant force patterns obtained from the front and rear are associated with different time steps, therefore there is no clear correlation between force patterns in the rear and in the front that generates the same DDP. Not only that, but the first few dominant force patterns in the front are very different from each other, the same thing applies to the rear of the vehicle.

Now that we are analyzing forces separately between front and rear we can try to understand better if there are similarities that could justify force patterns that are so different generating the same distortion pattern.

One initial approach is to compare the stress in some key points of the chassis between two different time steps belonging to the DDP. For the same time steps, we can also plot the displacement of the vehicle. For both cases a contour plot is probably the best visualization, results can be seen in the figures 3.22 and 3.23.

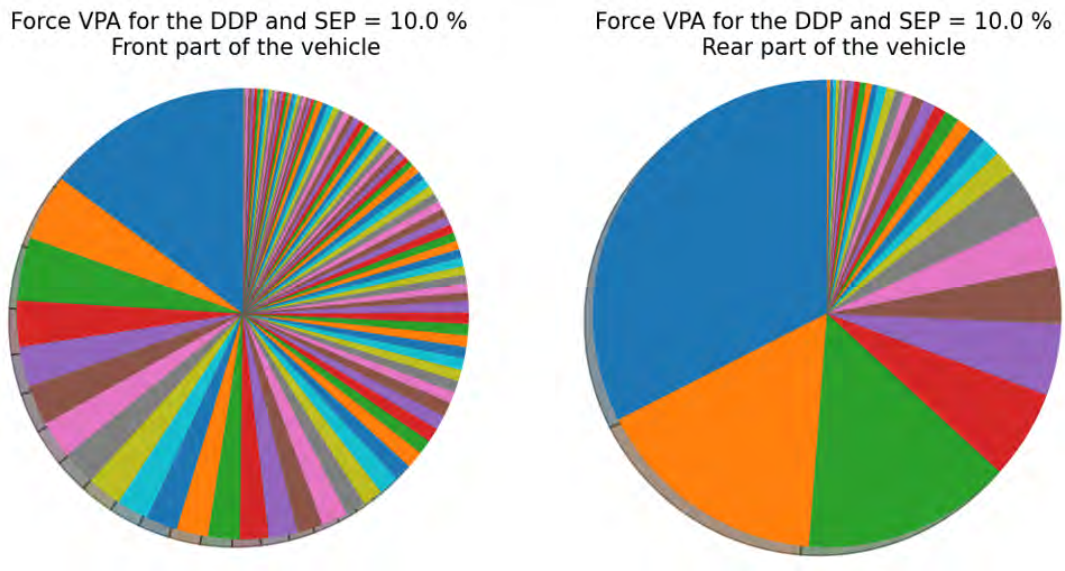

Figure 3.21: Force VPA Front and Rear separately. Shows that the force pattern, specially in the rear is not negligible, but is not as dominant as it was for the VPA of the distortions.

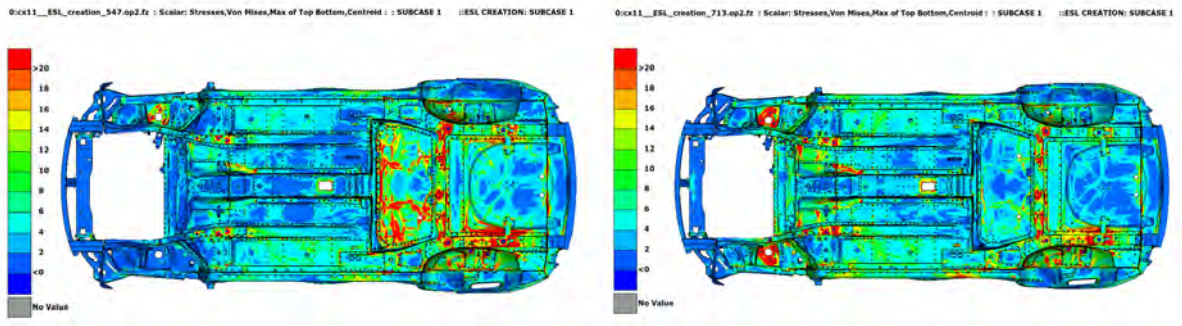

Figure 3.22: Stress in the chassis for two different time steps belonging to the DDP. Not only the stress is distributed very differently but some key points have huge differences, which is the case of the top mounts in the front of the vehicle.

Although the stress distribution is clearly different, especially in the top mounts, the displacement behavior is quite similar, this was also verified for other time steps belonging to the DDP. The indication that completely different force patterns can generate similar distortion patterns and displacement fields seems to be reasonable, but further analysis will be performed.

If we analyze the forces in figures 3.24 in the front for t equal to 1.18 seconds we will see that the lateral forces (Forces in the Y-direction) are not canceling each other in the knuckle, which is the two pairs of close points with approximately only lateral forces. For t equal to 0.84 seconds, there is some cancelation for the lateral forces, but nothing significant. On figure 3.25 we can see that there are no lateral forces, the modulus of the

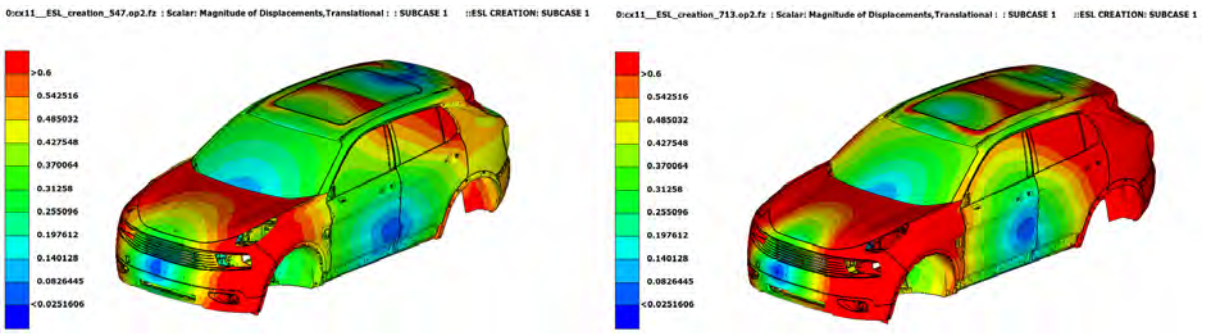

Figure 3.23: Displacements on the structure of the vehicle for the same time steps as figure 3.22. The displacement fields are similar, although the stress field was very different.

forces are reasonably small, but the result is in any case very different. Both time steps are associated with the DDP but both in the front and in the rear the difference between the forces are considerable.

What becomes clearer from this point of view is the moment that those forces are generating. In fact, when observing the results from the ESL and even the time steps from the modal transient analysis, the deformation of the structure as a whole resembles very much a pure torsion, with front and rear having opposite signs or one being reasonably higher than the other. Given these suspicious thoughts, a deeper understanding of the forces by relating the moment that is generated with the distortion of the openings is then performed.

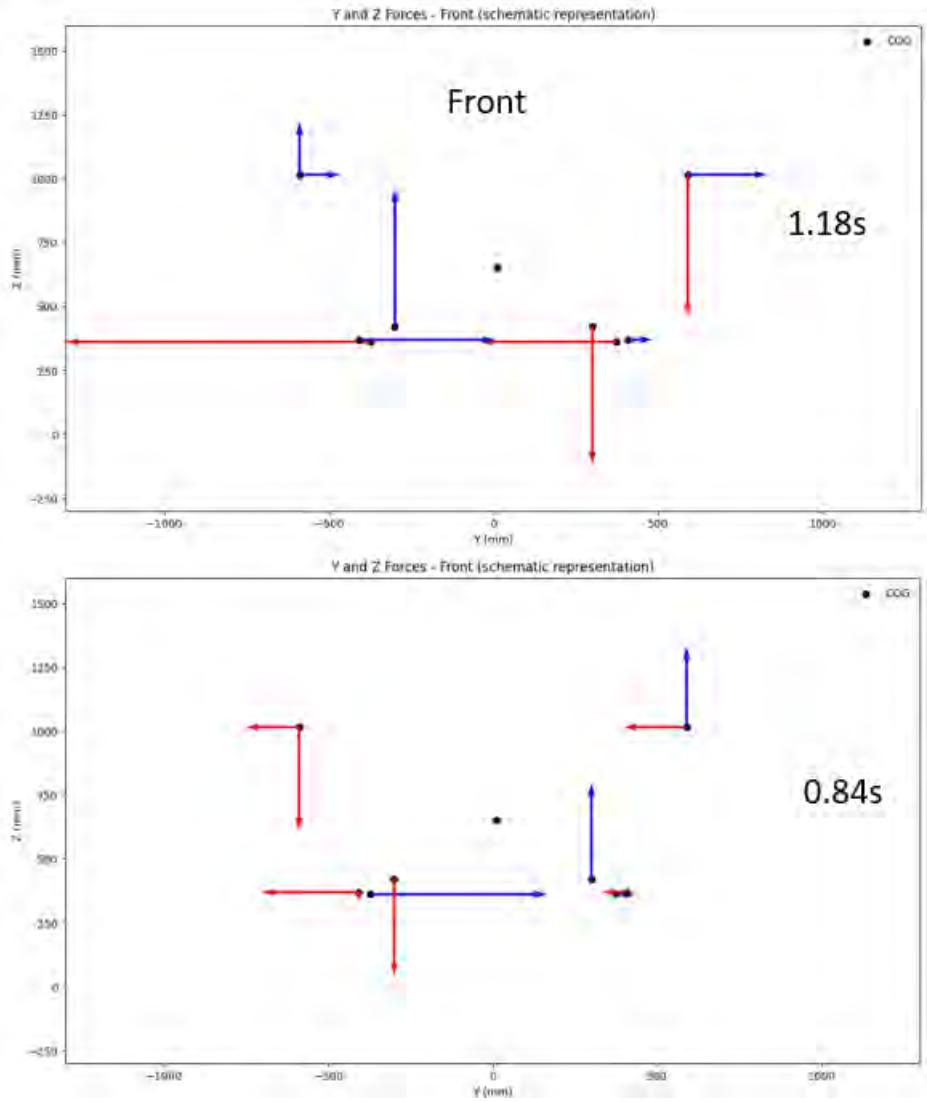

Figure 3.24: Forces in the front for two time steps with different force patterns. No significant canceling of lateral forces, meaning that they are not negligible. In any case, those time steps, although different are associated with the DDP.

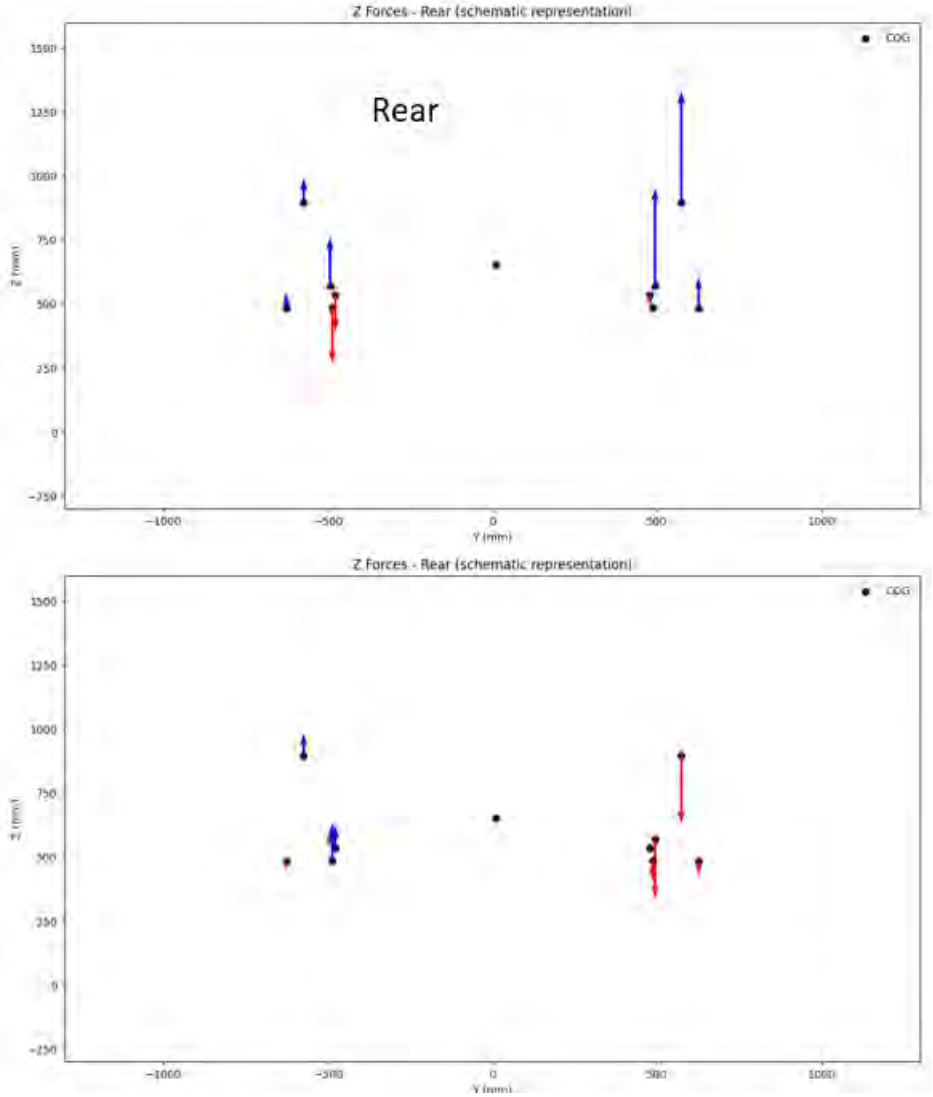

Figure 3.25: Forces in the rear for two time steps with different force patterns, for t = 1.18s and 0.84s, respectively, according to figure 3.24. Very different forces for both time steps, no lateral forces are present, yet they are both related to the DDP

3.7. Moment Analysis

The difference of the moment (the relative moment) around x, between the front and rear of the vehicle, can be seen in figures 3.26 and 3.27. Within the same plot, the relative moments are plotted but only for the time steps associated with the DDP associated with SEP equal to 20% and 5% respectively. The concentration of dots around the peaks of the continuous line (whole time history) is notorious and the suspicious of a relation between highest ODs (smaller SEP) and highest relative moment is obvious, this is even clearer in figure 3.27.

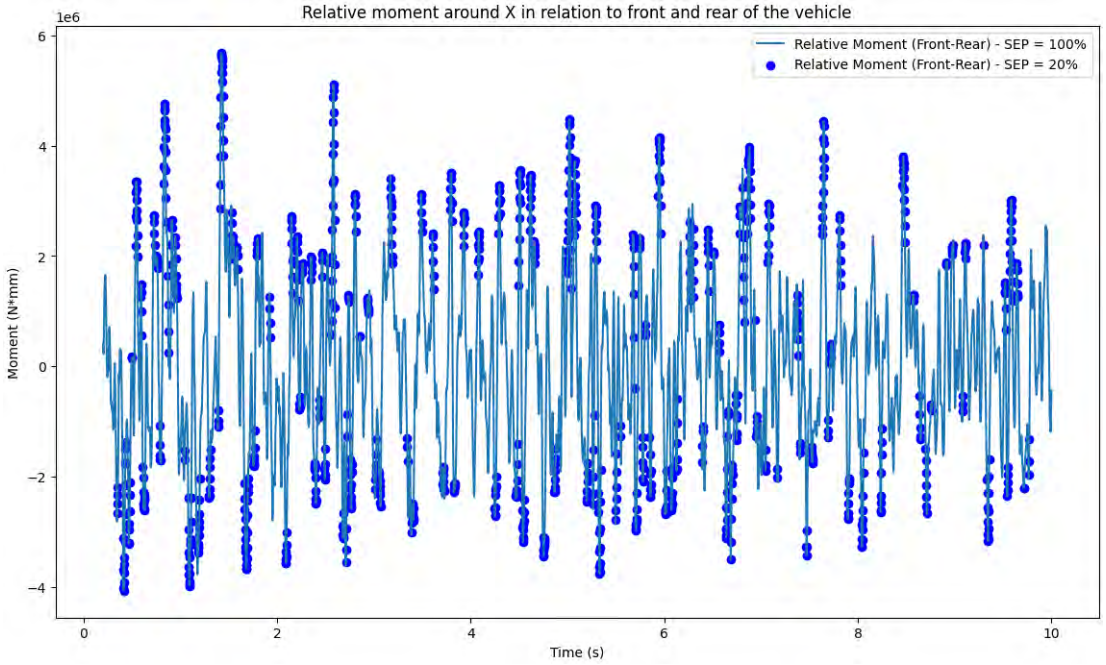

Figure 3.26: Relative moment around X for SEP equals to 100% (solid line, considering the whole time history) and to 20% (blue dots).

The continuous line is associated with all the time steps *i.e.* SEP equals 100%. The points for both figures 3.26 and 3.27 are associated with their respective SEP value, and it is clear that as SEP decreases, the high relative moments are becoming more and more relevant; therefore, there is a clear relation between high relative moments and the DDP. More than that, since only the highest distortion values are being plotted, if SEP is low, that means the high relative moment is also associated with the high overall distortions *i.e.* there is no relation of the DDP with the force patterns but with the moments generated by them.

Now the categories for each of the time steps used in figure 3.27 for SEP equal to 5% are used; results can be seen in figure 3.28, where category 1 and 2 are much more present

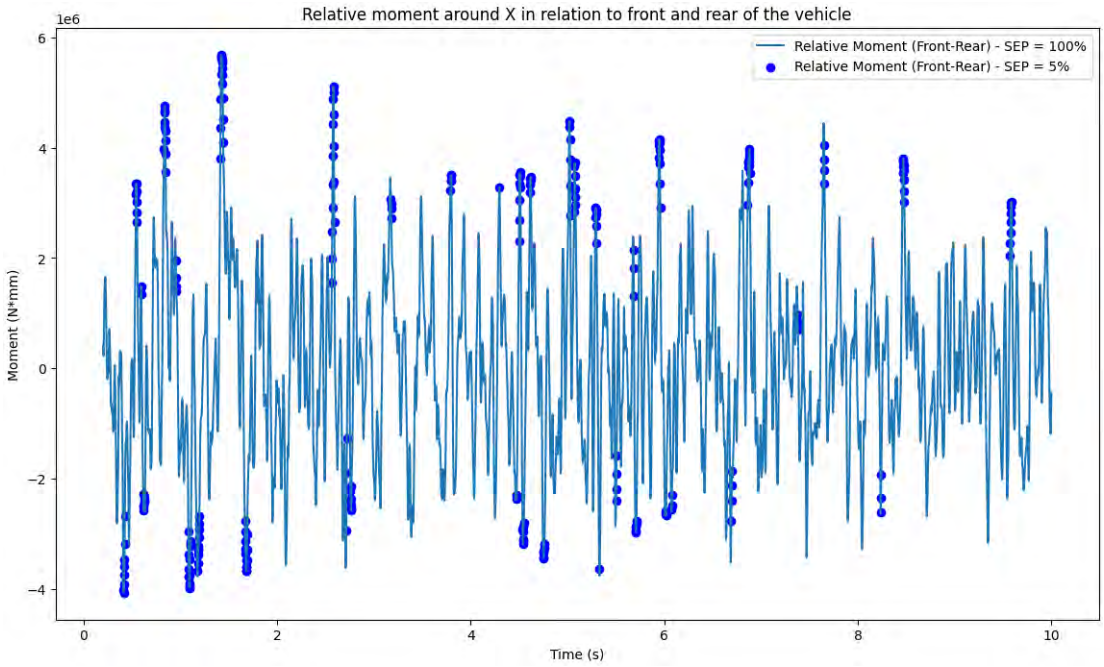

Figure 3.27: Relative moment around X for SEP equals to 100% (solid line, considering the whole time history) and to 5% (blue dots). There is a large presence of dots around the peaks of the relative moment, even more than in respect to figure 3.26,

than categories 3 and 4. This result is more clear in figure 3.29, where at 5% SEP the dominance of categories 1 and 2 are clear.

In theory, categories 2 and 3 seem similar, just changing which part of the vehicle has the highest moment (in magnitude), category 3 is however not so representative of any value of SEP, the conclusion is that the heavy weight of the motor is preventing the vehicle from twisting, therefore high distortions in the structure are unlikely, especially in the front of the vehicle.

What can be seen as well is that there are some consecutive time steps around most of the peaks of the relative moment graph (see figure 3.27), since we want to reduce the number of time steps so we end up with 1 to 4 ESLs in the end, it makes sense to use some strategies to achieve it. The procedure employed here is a type of clustering method, which consists of looking at each peak and among consecutive points only looking at those with high overall distortion, disregarding the others. Note that this is not the same clustering technique used in machine learning. The results, separating each peak by the category for SEP equal 100%, can be seen in figure 3.30.

We can also compare the results of figure 3.30, but only looking at the points representing each peak and the three highest distortions (throughout the whole time history, regardless

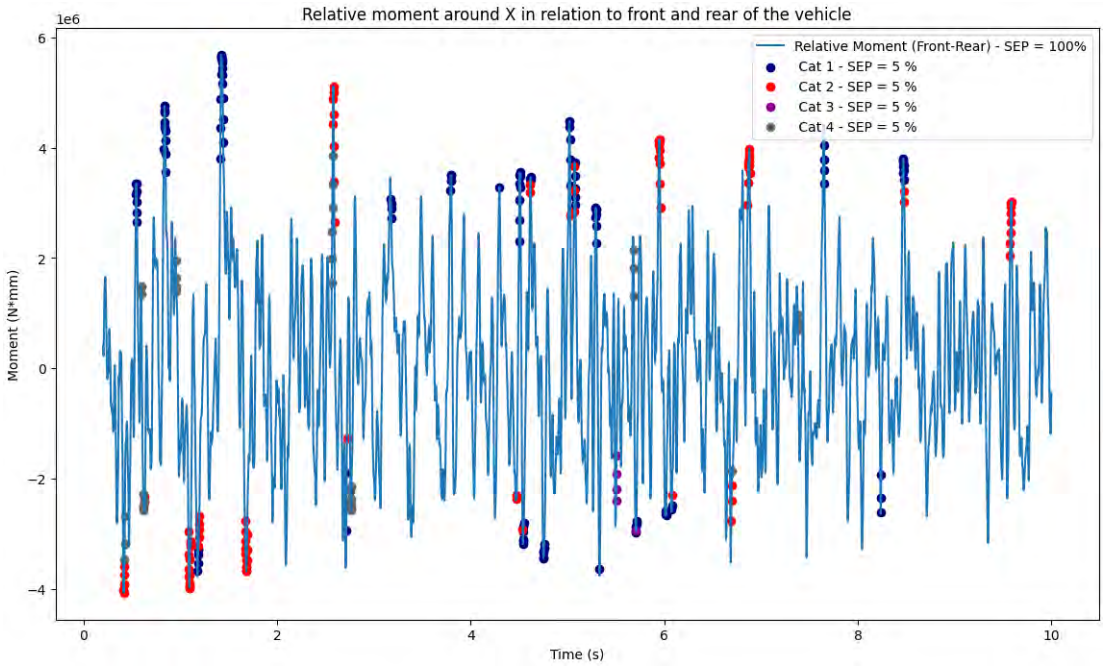

Figure 3.28: All categories for SEP = 5%. Categories 1 and 2 appears more often, specially when looking at the highest peaks of the relative moment.

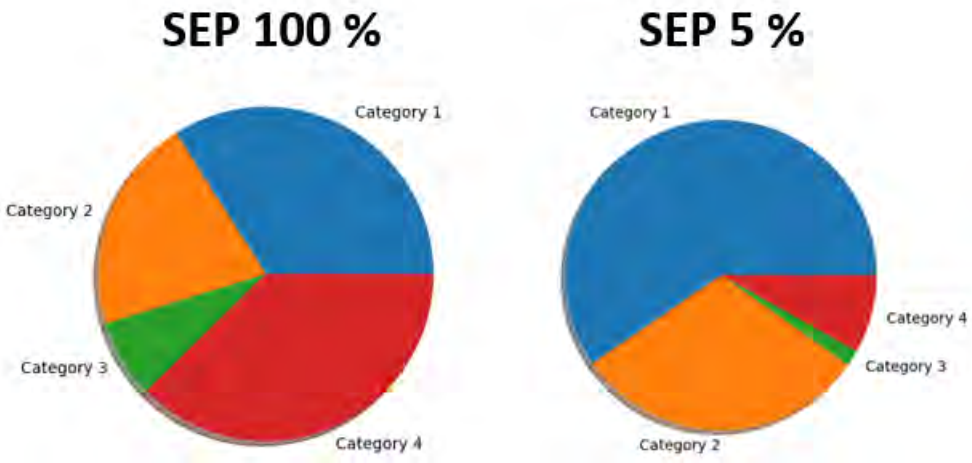

Figure 3.29: Categories for different SEPs. Showing the dominance of categories 1 and 2 as SEP decreases.

of whether they were or not present in the DDP), as mentioned in Section 3.5, results are shown in Figure 3.31.

It is clearly shown in figure 3.31 that the highest overall distortions are present when high relative moments occur and for low SEP, are also associated with the DDP as already shown beforehand. This is already a good indication that by looking at the relative moments and choosing a peak value we are likely capturing one of the most severe cases

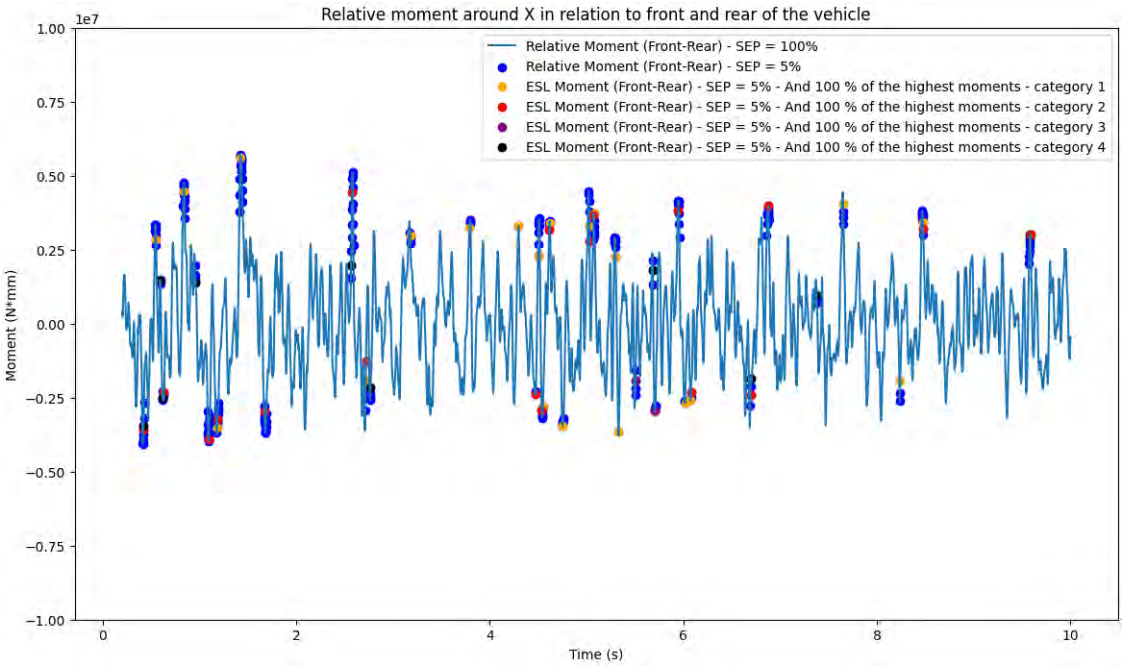

Figure 3.30: Clustering procedure. Every peak that is surrounded by blue dots is reduced to a single point, the color of this point is related with which moment category it belongs to.

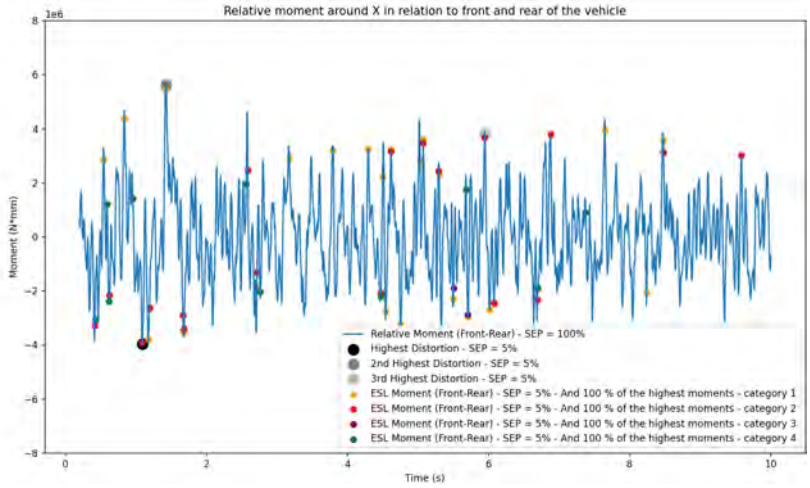

Figure 3.31: Relation of the relative moment with the highest distortions. Yellow and red dots are more present in the graph given the dominance of categories 1 and 2, the clustering method was also able to capture the highest ODs represented by the shades of gray dots.

in terms of overall distortion as well as representing the dominant distortion pattern, which is a specific type of torsion, in this case.

A step further is taken, since the goal is to be able to represent the most critical scenarios

while capturing the global behavior of the structure. A comparison between figures 3.26 and 3.27 shows that decreasing SEP will lead to higher relative moments, for the analyzed time steps, by considering the opposite *i.e.* focusing on higher relative moments, we aim to achieve the most critical scenarios, which are those with high overall distortions, Figure 3.31 is consistent with this line of thought.

This next step consisted of filtering figure 3.31 in a way that only the highest relative moment peaks are captured. 15% of the highest relative moment is used as a cutoff value, reducing from 49 points to 8. If 10% is used, we end up with only 5 points. Both results are shown in figures 3.32 and 3.33.

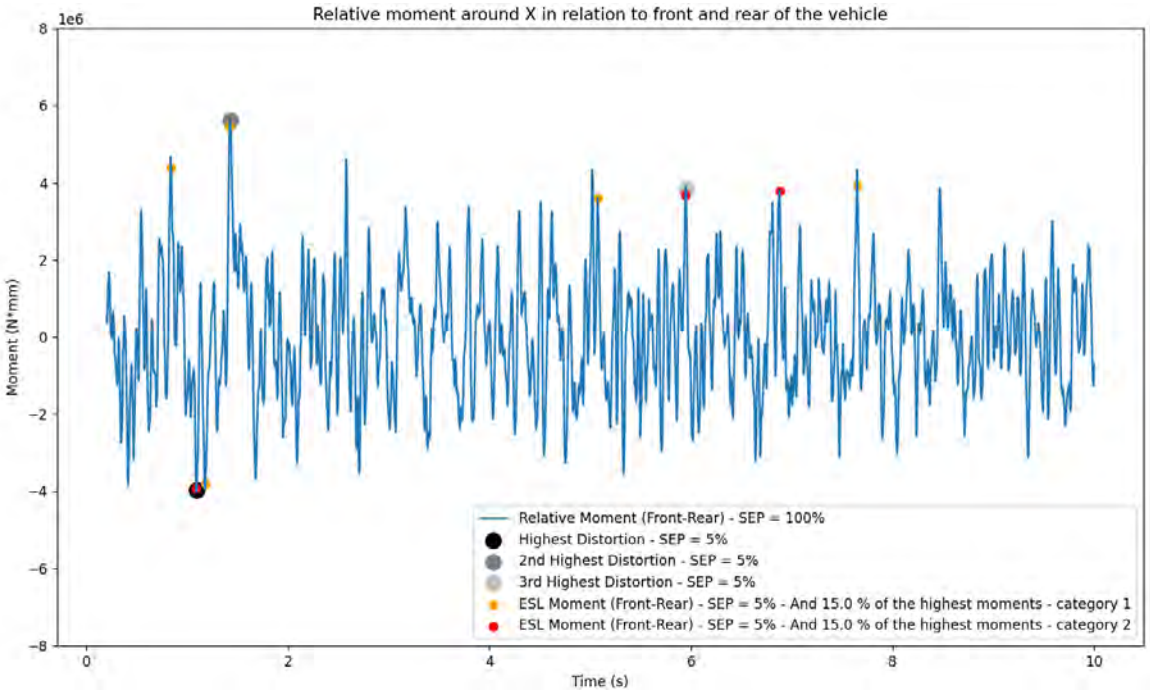

Figure 3.32: Relative moments with cutoff of 15% of maximum moment. At this point, we have removed all points from categories 3 and 4 while reducing the nuumber of points.

It should be noted that as mentioned already in this section, categories 1 and 2 are dominant, the non-appearance in figures 3.32 and 3.33 is due to the relative moments associated with all time steps of categories 3 and 4 not being high enough to surpass the cutoff value.

Once more, we have created ESLs (5 in this case) from figure 3.33, took the loads at that time step from the load history used in the dynamic simulation, ran 5 static analysis in parallel and compared them with the highest OD from the dynamic simulations with the ODFs for the 5 points from figure 3.33 (our proposed ESLs), results can be seen in figure 3.34.

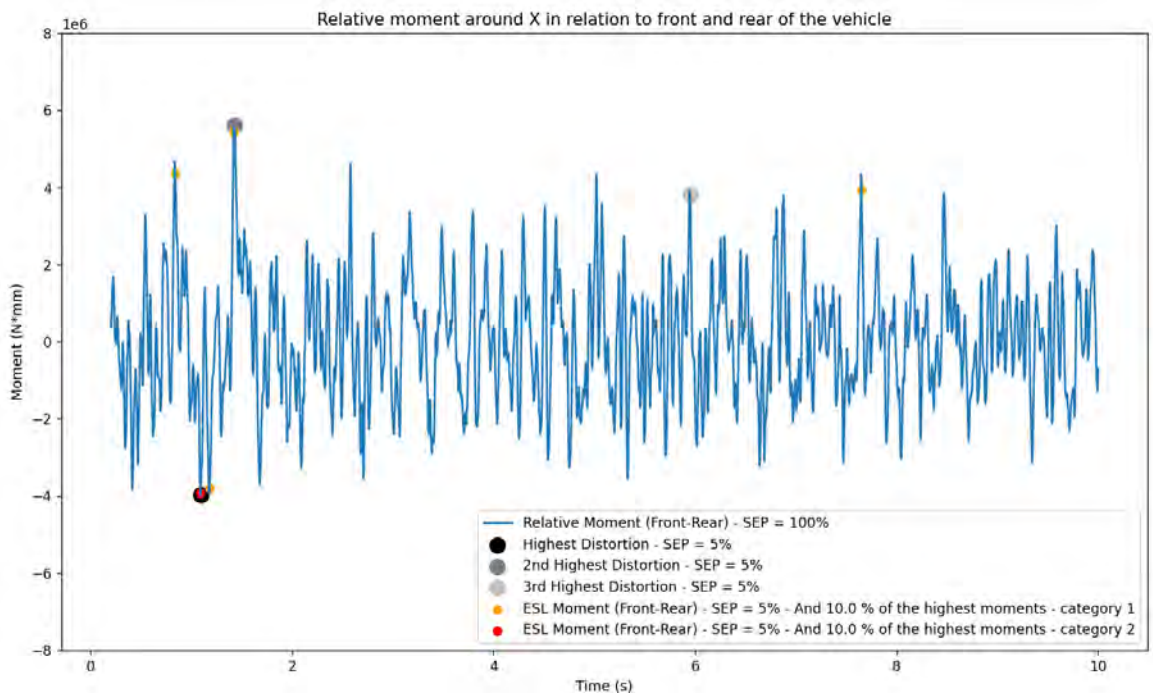

Figure 3.33: Relative moments with cutoff of 10% of maximum moment. Now only 5 points are present, still only categories 1 and 2 are present.

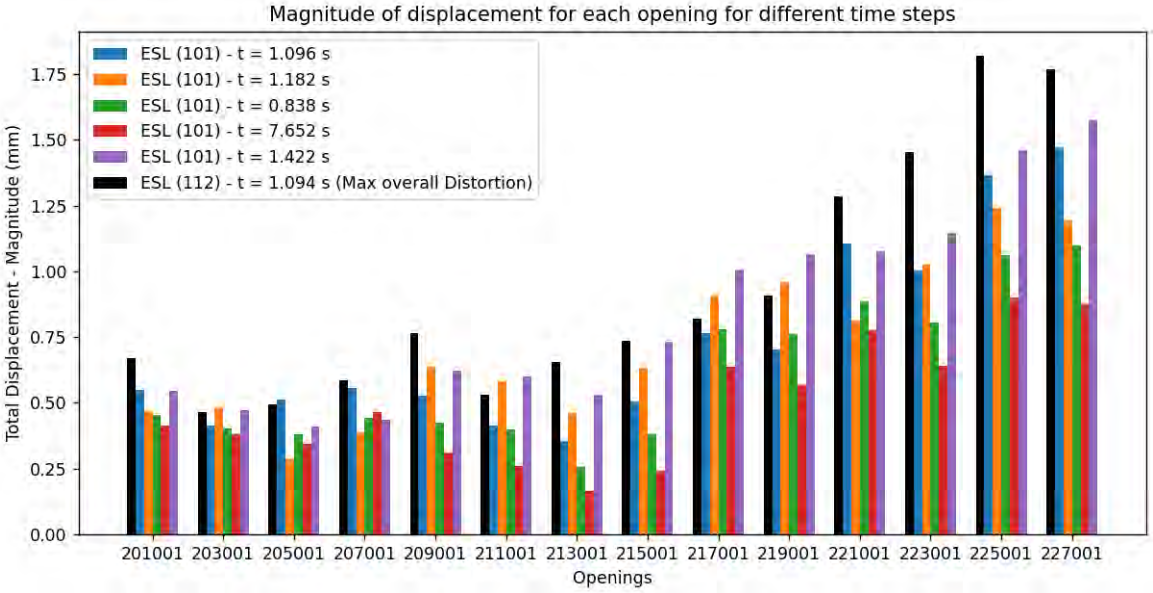

Figure 3.34: Comparison of ODFs for different ESLs against highest measured overall distortion from dynamic simulation.

It is clear from figure 3.34 that similarities were captured, although underestimating the values, nevertheless the behavior was indeed captured and even though the exact values were not matched, with 5 ESLs we managed to capture at least similar values for each

opening and be able to predict which time steps would lead to similar results, even before running a dynamic simulation. In fact, the time with the highest OD was 1.094 s (from the dynamic simulation) and one of the proposed ESL according to this work's methodology suggested 1.096 s, showing that it is accurate.

4 | Discussion

At the beginning of the work at CEVT, it seemed reasonable to assume that because there was a clear dominant distortion pattern maybe the forces would also generate a clear force pattern, which was not the case. The moment analysis was a strong approach that in theory can be applied to most conventional vehicles not only those developed by CEVT but its application to different types of vehicles are still being discussed and more work has to be done.

In fact, this approach was also used for an under-development vehicle called Zeekr (see 4.1), part of Waymo's fleet of autonomous taxis which is being developed by Geely, Waymo, Zeekr, and CEVT. A prototype of the Zeekr was presented publicly in 21^{st} November 2022 and consists of a fully electrical vehicle (EV). Given that the high mass of the engine is not present in an electric vehicle, the forces and global behavior responsible for twisting the body are not as straightforward as they were for a conventional vehicle; therefore, more detailed studies should be performed for this type of vehicle.

Figure 4.1: Prototype of Zeekr

One of the desired applications for this work would be to use the ESL for durability,

but given the non-similarity between the forces for the proposed ESLs, its application is limited.

The similarity of the forces that were related was the moment that they generated *i.e.* hundreds of different force patterns generated similar, in terms of magnitude, of relative moments which were responsible for twisting the vehicle generating the observed dominant distortion pattern, the torsion of the structure. Also, the influence of the center of rotation was not studied, once it was visually verified that it was not far from the COG of the vehicle.

After several modifications along the way, the final method consists of the following steps:

1. Calculate the distortions for all diagonals in the vehicle
2. Rank the distortions
3. Apply SEP (between 5% and 10% seems to work well for a conventional vehicle)
4. Perform PCA on distortions
5. Determine the distortion patterns
6. Remove the average value of the forces
7. Calculate relative moments for the whole time history
8. Use time steps obtained from DDP for the chosen SEP and plot their relative moment
9. Use the clustering method to reduce peaks to single points
10. Apply relative moment cutoff (10% to 30% seems to work well)
11. Retrieve the remaining time steps and the load cases associated with each one of them. Each load case represents an ESL

It is interesting to say that the proposed method is already being employed at CEVT for the development of Zeekr, although some changes have to be applied; however, the method will still be relevant for future applications, especially for Zeekr with the required updates in the method.

In this scenario, it seems relevant to propose some suggestions for future work:

- Consider other types of vehicles and understand if other behaviors different from a pure torsion are responsible for the DDP and how they can be included in the method.

- Propose modifications, such as including safety factors for forces that could lead to the use of a single ESL to be used for durability analysis.
- Improve MBS to obtain more accurate values for the forces in the engine mounts, as well as implement them in a continuation of this project, which could lead to more detailed results.

5 | Conclusion

It was verified that the assumption of quasi-static response was fulfilled; this led to an important numerical simplification, the simplification of a dynamic to a static simulation, saving hours of computational time for all of the development phases of the vehicle.

Obtaining a few ESLs instead of a single one was not the initial goal, but showed to be reasonable given the huge different combination of forces that would generate similar events.

The proposed method also improved in terms of accuracy, time consumption, and complexity of the loads (16 instead of 4) with respect to the state-of-the-art method, besides that, no target for optimization is required, meaning that an ESL (or a few) can be obtained without initial assumptions or target values for optimization procedures.

The proposed methodology also answer and improves the key points presented in the state-of-the-art chapter:

- The high relative moments were indeed responsible for high overall distortions and for the global behavior of the vehicle *i.e.* the Dominant Distortion Pattern.
- There is no oversimplification of the force locations, since all of them are being considered
- There is no need to run a simulation beforehand to anticipate which loads to use to obtain the highest overall distortions, ESLs can be obtained straight away from the load history after a short moment analysis with a python script, as the time required to run the scripts was not greater than 5 minutes

Other two significant gains of this procedure are that by obtaining multiple ESLs that consider high forces there is a better understanding of localized stresses in the structure, very relevant from a durability point of view, besides that 5 ESLs can be run in parallel and are much less time consuming than a modal transient analysis, taking up to 95% less computational time.

The applicability of this work is already taken place, with the assistance of coworkers at

CEVT it was implemented in META, a post-processing software, and is already in use. Future work is still necessary to be able to implement such an efficient and not-time-consuming method, but satisfactory results so far lead to believe that the right path is being trailed.

Bibliography

[1] D. N. Alam and V. Chennubhotla. Use of cae tool to evaluate the body pressure distribution plot on automotive seating. Technical report, SAE Technical Paper, 2019.

[2] K.-J. Bathe. *Finite element procedures*. Klaus-Jurgen Bathe, 2006.

[3] X. Chen and A. Kareem. Equivalent static wind loads for buffeting response of bridges. *Journal of Structural Engineering*, 127(12):1467–1475, 2001.

[4] X. Chen and A. Kareem. Equivalent static wind loads on buildings: New model. *Journal of Structural Engineering*, 130(10):1425–1435, 2004.

[5] W.-S. Choi and G. Park. Transformation of dynamic loads into equivalent static loads based on modal analysis. *International Journal for Numerical Methods in Engineering*, 46(1):29–43, 1999.

[6] W.-S. Choi and G.-J. Park. Structural optimization using equivalent static loads at all time intervals. *Computer methods in applied mechanics and engineering*, 191 (19-20):2105–2122, 2002.

[7] L. Gu and R. Yang. Cae model validation in vehicle safety design. Technical report, SAE Technical Paper, 2004.

[8] H. Hotelling. Analysis of a complex of statistical variables into principal components. *Journal of educational psychology*, 24(6):417, 1933.

[9] F. Huizinga, R. Van Ostaijen, and A. Van Oosten Slingeland. A practical approach to virtual testing in automotive engineering. *Journal of Engineering Design*, 13(1): 33–47, 2002.

[10] H.-H. Jang, H. Lee, J. Lee, and G. Park. Dynamic response topology optimization in the time domain using equivalent static loads. *AIAA journal*, 50(1):226–234, 2012.

[11] S. Jeong, S. Yi, C. Kan, V. Nagabhushana, and G. Park. Structural optimization of an automobile roof structure using equivalent static loads. *Proceedings of the*

Institution of Mechanical Engineers, Part D: Journal of Automobile Engineering, 222(11):1985–1995, 2008.

[12] H. Kanchwala and A. Chatterjee. Adams model validation for an all-terrain vehicle using test track data. *Advances in Mechanical Engineering*, 11(7):1687814019859784, 2019.

[13] B. Kang, W. Choi, and G. Park. Structural optimization under equivalent static loads transformed from dynamic loads based on displacement. *Computers & Structures*, 79(2):145–154, 2001.

[14] B.-S. Kang, G. Park, and J. Arora. Optimization of flexible multibody dynamic systems using the equivalent static load method. *AIAA journal*, 43(4):846–852, 2005.

[15] K.-J. Kim, J.-H. Lim, J.-H. Park, B.-I. Choi, J.-W. Lee, and Y.-J. Kim. Light-weight design of automotive aa6061 rear sub-frame based on cae simulation. *Transactions of the Korean Society of Automotive Engineers*, 20(3):77–82, 2012.

[16] V. Lakshminarayan, H. Wang, W. Williams, Y. Harajli, and S. Chen. Application of cae nonlinear crash analysis to aluminum automotive crashworthiness design. Technical report, SAE Technical Paper, 1995.

[17] D.-C. Lee and C.-S. Han. Cae (computer aided engineering) driven durability model verification for the automotive structure development. *Finite Elements in Analysis and Design*, 45(5):324–332, 2009.

[18] D.-G. Lee, J.-M. Hong, and J. Kim. Vertical distribution of equivalent static loads for base isolated building structures. *Engineering Structures*, 23(10):1293–1306, 2001.

[19] J.-J. Lee, U.-J. Jung, and G.-J. Park. Shape optimization of the workpiece in the forging process using equivalent static loads. *Finite Elements in Analysis and Design*, 69:1–18, 2013.

[20] Y. Lee, J.-S. Ahn, and G.-J. Park. Crash optimization of an automobile frontal structure using equivalent static loads. *Transactions of the Korean Society of Automotive Engineers*, 23(6):583–590, 2015.

[21] K. Li and S. Ren. Strength and fatigue analysis for automotive pedal based on cae. In *Second International Conference on Mechanic Automation and Control Engineering*, pages 5243–5246, 2011.

[22] M. J. Moeller, R. S. Thomas, H. Maruvada, N. S. Chandra, and M. Zebrowski. An

assessment of a fea nvh cae body model for design capability. Technical report, SAE Technical Paper, 2001.

[23] G. Park and B. Kang. Validation of a structural optimization algorithm transforming dynamic loads into equivalent static loads. *Journal of optimization theory and applications*, 118(1):191–200, 2003.

[24] G.-J. Park. Technical overview of the equivalent static loads method for non-linear static response structural optimization. *Structural and Multidisciplinary Optimization*, 43(3):319–337, 2011.

[25] K. Pearson and O. Lines. Planes of closest fit to systems of points in space. *Lond. Edinb. Dublin Philos. Mag. J. Sci*, 2:559–572, 1901.

[26] R. Ramkumar, Y. Surkutwar, A. Subbarao, N. Karanth, S. Sawant, and P. Kulkarni. An investigation of vibration characteristics in automotive seats using experimental and cae techniques. Technical report, SAE Technical Paper, 2011.

[27] M.-K. Shin, K.-J. Park, and G.-J. Park. Optimization of structures with nonlinear behavior using equivalent loads. *Computer Methods in Applied Mechanics and Engineering*, 196(4-6):1154–1167, 2007.

[28] H. Su. Cae virtual durability tests of automotive products in the frequency domain. *SAE International Journal of Passenger Cars-Mechanical Systems*, 1(2008-01-0240): 165–174, 2008.

[29] H. Su, J. Kempf, B. Montgomery, and R. Grimes. Cae virtual test of air intake manifolds using coupled vibration and pressure pulsation loads. *SAE transactions*, pages 953–961, 2005.

[30] J. Wannenburg, P. S. Heyns, and A. D. Raath. Application of a fatigue equivalent static load methodology for the numerical durability assessment of heavy vehicle structures. *International Journal of Fatigue*, 31(10):1541–1549, 2009.

[31] J. Weber, P. Sabiniarz, C. Wickman, L. Lindqvist, and R. Söderberg. Squeak&rattle simulation at volvo car corporation using the e-line™ method. In *5th ANSA & μeta International Conference*, 2013.

[32] J. Weber, V. Jönsson, L. Hansson, R. Varela, and B. Käck. Opening distortion fingerprint (odf)-a new body evaluation method for perceived quality and vehicle dynamics. Technical report, SAE Technical Paper, 2022.

[33] J. Will. State of the art–robustness evaluation in cae-based virtual prototyping

processes of automotive applications. *Proceedings Optimization and Stochastic Days*, 4, 2007.

[34] S. Yi, J. Lee, and G. Park. Crashworthiness design optimization using equivalent static loads. *Proceedings of the Institution of Mechanical Engineers, Part D: Journal of automobile engineering*, 226(1):23–38, 2012.

A | Appendix A

A.1. PCA

Principal Component Analysis (PCA) is a technique commonly used to reduce noise or dimension in a dataset while maintaining the highest variance due to patterns in it. This method relies on reducing a vector of data of higher dimensions to 1,2 or 3 dimensions, when convenient, allowing a better understanding of the distribution of the points.

The origins of PCA can be traced back to Pearson [25], but the modern theory was formed by Hotelling [8]. The PCA targets the greatest variances and divides them into principal components, where the highest variance is associated with the principal component, the second highest to the second principal component, and so on.

The procedure of the PCA can be promptly described below:

1. Standardize the dataset: This avoids having outliers or large numbers having great impact in the overall result.
2. Calculate the covariance matrix of the dataset.
3. Calculate the eigenvalues and associated eigenvectors for the covariance matrix.
4. Sort the eigenvalues and their respective eigenvectors
5. Choose the desired highest principal directions, the amount that better satisfies your need to understand the data
6. Transform the original matrix